Computer Networks 115 (2017) 65–81

Contents lists available at ScienceDirect

Computer Networks

journal homepage: www.elsevier.com/locate/comnet

Quantifying inhomogeneity of spatial point patterns

Udo Schilcher[a,b,*], Günther Brandner[b], Christian Bettstetter[a,b]

[a] University of Klagenfurt, Lakeside B02, 9020 Klagenfurt, Austria
[b] Lakeside Labs GmbH, Lakeside B04, 9020 Klagenfurt, Austria

ARTICLE INFO

Article history:
Received 3 August 2016
Revised 9 December 2016
Accepted 30 December 2016
Available online 10 January 2017

Keywords:
Wireless networks
Simulation
Modeling
Inhomogeneous spatial distribution
Inhomogeneity measure

ABSTRACT

This article compares *measures for quantifying the level of inhomogeneity* of a given spatial point pattern. Comparisons are based on two main metrics: first, we evaluate the performance of the measures on both certain stochastic point processes and on very specific point patterns designed to expose potential weaknesses of the inhomogeneity measures. Second, we evaluate the computational complexity of the measures. Results show that choosing a measure is a tradeoff between accurate assessment of inhomogeneity and computational complexity. The only exception is the proposed *extended wrap-around measure*, which is performing well in terms of both metrics.

1. Motivation and contributions

Stochastic models for the spatial distribution of nodes are used in simulation and analysis of wireless networks. Most publications employ nodes that are *homogeneously* distributed at random — either sampling from a uniform distribution on a given area (see illustration in Fig. 1(a)) or applying a Poisson point process in case of an infinite area. It is rarely taken into account that node locations in the real world are often *inhomogeneously* distributed (Fig. 1(b)), due to the fact that devices are concentrated in hotspots, such as buildings, malls, and pedestrian zones or because users move along movement paths. This methodological lack exists despite the fact that important performance measures, such as system capacity and connectivity, heavily depend on the node distribution (see, e.g., [1–6]).

There are several reasons as to why inhomogeneous node distributions are hardly used. A first reason is that the use of inhomogeneous locations makes performance analysis more complex. Homogeneous distributions have well-known stochastic properties (e.g., with respect to distances between nodes [7,8]), which make mathematical derivations of performance measures feasible. In simulation-based work, standard software tools offer homogeneous distributions but often lack inhomogeneous ones.

A second reason is that the research community has no common approach for generating inhomogeneous node distributions. There are some papers suggesting and using different approaches (see, e.g., [9–11]), but none of them has become a reference model, neither by agreement in the community nor by "natural selection." This lack of standardized methodology makes it difficult to compare performance results that use inhomogeneous distributions. It is worth mentioning that the development was different in mobility modeling, where the random waypoint model [12] has been used by the majority of publications on ad hoc networks over many years and thus has acted as a reference model — a *de facto* standard that has been used in hundreds of simulations and whose stochastic properties, advantages, and pitfalls have been investigated in a comprehensive manner (see, e.g., [13–18]).

A third reason as to why inhomogeneous node distributions are rarely used is the fact that the term "inhomogeneous" has not been quantified in the wireless networks literature, i.e., there is no accepted metric for the *level of inhomogeneity* in a given node pattern. Without having such a metric, no generalization of performance results to a higher degree of abstraction is possible, but results will only be valid for the particular scenario under investigation. A similar situation holds in mobility modeling, where attempts were made to quantify the level of mobility (see, e.g., [19,20]).

This paper intends to contribute toward solving the third issue. We discuss and present methods for quantifying the inhomogeneity of a spatial node pattern, continuing and significantly extending our first approach in this direction [21]. These methods are called *inhomogeneity measures* in the following. Our overall objective is to

* Corresponding author.
E-mail addresses: udo.schilcher@aau.at (U. Schilcher), guenther.brandner@me.com (G. Brandner), christian.bettstetter@aau.at (C. Bettstetter).

http://dx.doi.org/10.1016/j.comnet.2016.12.018

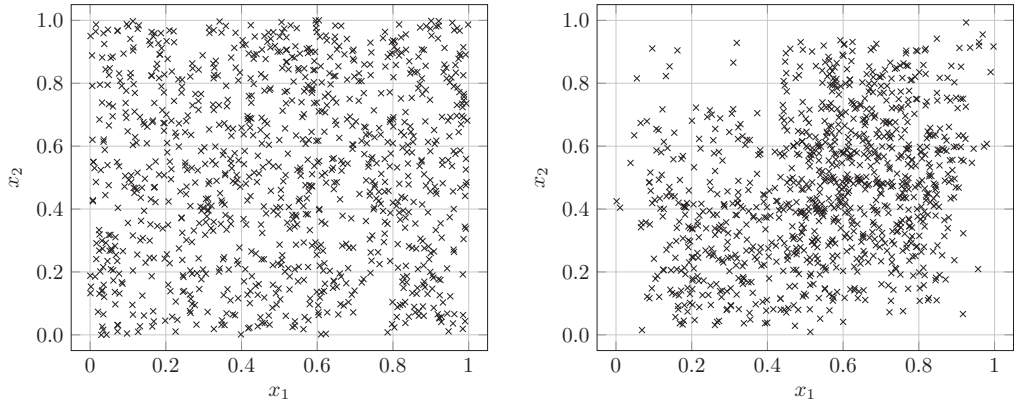

(a) An almost homogeneous point pattern (b) An inhomogeneous point pattern

Fig. 1. Two-dimensional point patterns with 1 000 points.

obtain an inhomogeneity measure that is invariant against translation and rotation of the pattern and independent on the total number of nodes. Furthermore, the computational complexity in calculating the inhomogeneity should be low.

The terms “node” and “point” are used interchangeably; the term “node” is common in the literature on wireless networks and graph theory; the term “point” is common in spatial statistics.

The contributions of this article are as follows:

- We extend Ripley’s K-function known from the field of stochastic geometry [22,23] for assessing local deviations from homogeneity in spatial point patterns to yield a global inhomogeneity measure.
- We extend discrepancy measures commonly used in the field of numerical integration and statistical testing and apply them as inhomogeneity measures.
- We evaluate and compare inhomogeneity measures with respect to their ability to assess the inhomogeneity of spatial point patterns and with respect to their computational effort.
- We propose a new inhomogeneity measure, the Extended Wrap-Around Inhomogeneity Measure, combining computational efficiency and good capability to assess the inhomogeneity of spatial point patterns.
- We present an algorithm to generate spatial point patterns exhibiting specified inhomogeneity.

Let us give examples as to how inhomogeneity measures can be applied in the analysis of wireless networks: Firstly, they can be adopted to evaluate the performance of cooperative diversity in wireless networks [24]. The reason for the importance of such evaluations is that the performance of cooperative diversity is significantly influenced by the spatial characteristics of the network [25]. This can also be seen when varying the distances between nodes in a cooperative relaying setup [26]: Performance is changed in a non-trivial way showing interdependence between spatial characteristics and other parameters like channel quality. Further, the analysis of wireless networks modeled via a Ginibre point process [27] resembles a more realistic model than Poisson point processes for many application scenarios incorporating different levels of inhomogeneity. The derivation of the expected interference in networks modeled by hard-core processes [28] is an example, in which inhomogeneity plays an important role. The performance analysis of femtocell access point deployment [29], and the investigation of SIR asymptotics under very general modeling assumptions including inhomogeneously distributed nodes [30] are further examples that show that the inhomogeneity of point patterns is an important parameter that has to be considered for a comprehensive analysis of wireless networks.

The remainder of this manuscript is organized as follows: Section 2 presents definitions and introduces the notation used throughout this manuscript. Section 3 presents methods for assessing the (in-)homogeneity of spatial point patterns and proposes the *extended wrap-around inhomogeneity measure*. Section 4 evaluates these methods with respect to their ability to assess inhomogeneity and their computational effort. Finally, Section 5 presents an algorithm for generating spatial point patterns with specified inhomogeneity values. Section 6 presents related work, and Section 7 concludes this manuscript.

2. Definitions and notation

2.1. Definitions from geometry

The Euclidean distance between two points $\vec{x}, \vec{y} \in \mathbb{R}^D$ in a D-dimensional space with $D \in \mathbb{N}$ is given by

$$d_{\vec{x}\vec{y}} = d(\vec{x}, \vec{y}) = \sqrt{\sum_{d=1}^{D} (x_d - y_d)^2},$$

where x_d and y_d are the dth components of $\vec{x}$ and $\vec{y}$, respectively (see [31], p. 94).

Let $\mathcal{U} \subseteq \{1, 2, \ldots, D\}$ be a nonempty subset of the set of all natural numbers up to D. The projection of $\vec{x}$ onto $\mathcal{U}$ is $\vec{x}^{\mathcal{U}} = (x_u)_{u \in \mathcal{U}} = (x_{u_1}, x_{u_2}, \ldots, x_{u_K})$ for $\mathcal{U} = \{u_1, u_2, \ldots, u_K\}$ and $u_1 < u_2 < \ldots < u_K$. The projection $\mathcal{S}^{\mathcal{U}}$ of a set $\mathcal{S}$ of points onto $\mathcal{U}$ is

$$\mathcal{S}^{\mathcal{U}} = \{\vec{x}^{\mathcal{U}} \mid \vec{x} \in \mathcal{S}\}.$$

Let $|\mathcal{S}|$ denote the number of elements of $\mathcal{S}$.

An (open) ball $B(\vec{x}, r)$ with radius r centered in $\vec{x}$ is defined as

$$B(\vec{x}, r) = \{\vec{y} \in \mathbb{R}^D \mid d_{\vec{x}\vec{y}} < r\}.$$

We say that $\vec{x} < \vec{y}$ and $\vec{x} \leq \vec{y}$ if and only if $x_d < y_d$ and $x_d \leq y_d$ for all $1 \leq d \leq D$, respectively.

Let $\bigtimes_{u \in \mathcal{U}}^{<} \mathcal{A}_u$ define the ordered Cartesian product on $\mathcal{U} = \{u_1, u_2, \ldots, u_K\}$:

$$\bigtimes_{u \in \mathcal{U}}^{<} \mathcal{A}_u = \bigtimes_{k=1}^{K} \mathcal{A}_{u_k}.$$

The orthotope determined by the vectors $\vec{x}^{\mathcal{U}}$ and $\vec{y}^{\mathcal{U}}$, $\vec{y}^{\mathcal{U}} > \vec{x}^{\mathcal{U}}$ is

$$O(\vec{x}^{\mathcal{U}}, \vec{y}^{\mathcal{U}}) = \bigtimes_{u \in \mathcal{U}}^{<} [x_u, y_u].$$

The volume of $O(\vec{x}^{\mathcal{U}}, \vec{y}^{\mathcal{U}})$ is denoted as $V(O(\vec{x}^{\mathcal{U}}, \vec{y}^{\mathcal{U}}))$.

Finally, the modulo operation on a vector $\vec{x} = (x_1, x_2, \ldots, x_D)$ is defined as

$$(x_1, x_2, \ldots, x_D) \bmod b = (x_1 \bmod b, x_2 \bmod b, \ldots, x_D \bmod b).$$

2.2. Spatial homogeneity and inhomogeneity

A stochastic process generating a spatial point pattern is said to exhibit *complete spatial randomness* (CSR) if the number of points in any orthotope O follows a Poisson distribution with mean $\lambda V(O)$ or, equivalently, if all points in O are independent random samples from the uniform distribution on O [32]. Based on this definition from the applied statistics literature, we define homogeneity of a point pattern as follows.

A spatial point pattern $\mathcal{S}$ is completely *homogeneous* if there is a single parameter λ such that for every O in $\mathbb{R}^D$ the number of points contained in O is $\lambda\, V(O)$. The more the spatial point pattern deviates from this condition, the more *inhomogeneous* the pattern is. A pattern is completely inhomogeneous if all points are at the same location.

A stationary Poisson point process (PPP) with intensity λ on a finite area would yield, with high probability and on average, spatial point patterns that are almost homogeneous in a certain volume. The proportionality constant is not exactly the same for all O, but there is, with high probability, an interval $[\lambda - \varepsilon, \lambda + \varepsilon]$ where all such constants are contained.

2.3. Restriction to two dimensions and unit area

This paper considers spatial point patterns in two dimensions. In this case, a point is $\vec{x} = (x_1, x_2) \in \mathbb{R}^2$, and a ball $B(\vec{x}, r)$ is a circle around $\vec{x}$ with radius r. Since $\mathcal{U} \subseteq \{1, 2\}$, the orthotope $O(\vec{x}^{\mathcal{U}}, \vec{y}^{\mathcal{U}})$ is a rectangle or line, and the volume $V(O(\vec{x}^{\mathcal{U}}, \vec{y}^{\mathcal{U}}))$ is an area or length.

Furthermore, we consider a finite number of points in the unit square $C = [0, 1]^2$, i.e., $\mathcal{S} \subset C$. We consider $\mathcal{S}$ to be a multiset, i.e., points can occur multiple times in $\mathcal{S}$. The restriction to the unit square is made without loss of generality, since every point pattern on a rectangular area can be mapped to the unit square by linear transformations [33]. The number of points is denoted by $N = |\mathcal{S}|$.

3. Inhomogeneity measures

This section addresses three classes of inhomogeneity measures (IMs) and proposes extensions to assess the level of inhomogeneity of a given spatial point pattern on a finite area using a standardized value range [0, 1] for the level of inhomogeneity. A spatial point pattern with IM close to 0 is very homogeneous; a pattern with IM close to 1 is very inhomogeneous.

The first IM is based on Ripley's K-function. The K-function assesses local inhomogeneities from which we derive a global measure for inhomogeneity. The second class of IM are discrepancy measures commonly applied in the fields of statistical testing and numerical integration. These measures, as proposed in literature, do not use a standardized value range. Thus, we normalize existing discrepancy measures to fit the intended value range. Further, we introduce the *extended wrap around IM* as an extension of one of these measures. The third class is a novel grid-based IM. A preliminary version of this IM was proposed by some of the authors of this manuscript in [21].

3.1. Inhomogeneity measure based on Ripley's K-function

3.1.1. Definition of the K-function

Ripley's K-function proposed in [22] and [23] is widely used in statistics to detect local deviations from homogeneity in a spatial point pattern. The idea is that for a stationary PPP with intensity λ the expected number of points of the point pattern within a circle $B(\vec{x}, r)$ centered at an arbitrary point $\vec{x} \in \mathbb{R}^2$ is proportional to $r^2\pi$, i.e.,

$$\frac{|\mathcal{S}_\infty \cap B(\vec{x}, r)|}{r^2\pi} \approx \lambda,$$

where $\mathcal{S}_\infty$ denotes a realization of the PPP on $\mathbb{R}^2$. Hence, plotting the number of points $|\mathcal{S}_\infty \cap B(\vec{x}, r)|$ over r leads to a curve that closely resembles the function $r \mapsto r^2\pi\lambda$. In contrast, there would be a large difference between these two functions for inhomogeneous patterns.

3.1.2. Relation to pair-correlation functions

A measure often used in statistics to describe the second-order behavior of a point process is the *pair-correlation function* $g(r)$. It has a strong connection to Ripley's K-function, given by

$$g(r) = \frac{\frac{\mathrm{dK}(r)}{\mathrm{dr}}}{2r\pi}.$$

Hence, in principal one could apply the K-function and the pair-correlation function for the same purpose; which function to choose depends mainly (although not only) on the ease of applying them [34]. In our case, we could define an inhomogeneity measure based on both of them. For the K-function, we measure the distance between the empirical $K(r)$ and $r^2\pi$, where $r^2\pi$ is the K-function of the stationary Poisson point process. In case of the pair-correlation function, we would measure the deviation of the empirical $g(r)$ from 1, the latter being $g(r)$ for the stationary PPP. Since the resulting inhomogeneity values are not expected to differ significantly for $K(r)$ and $g(r)$, we solely define an inhomogeneity measure based on $K(r)$.

3.1.3. Application to finite point patterns

The K-function can also be applied to finite point patterns $\mathcal{S}$ on C. An estimator for the K-function is (see [35], pp. 639–640)

$$\widehat{K}(r, \mathcal{S}) = \frac{1}{N\widehat{\lambda}} \sum_{\vec{x}, \vec{y} \in \mathcal{S}}^{\neq} \frac{1}{w(\vec{x}, \vec{y})} \mathbf{1}_r(d_{\vec{x}\vec{y}}),$$

where $\widehat{\lambda} = \frac{N}{V(C)} = N$ is an estimate of λ,

$$\mathbf{1}_r(d_{\vec{x}\vec{y}}) = \begin{cases} 1 & \text{if } d_{\vec{x}\vec{y}} < r \text{ and} \\ 0 & \text{else,} \end{cases}$$

is an indicator function, and $w(\cdot, \cdot)$ is a weighting function for border correction.

The weighting function is important because the observation area C has borders. It is defined to be the fraction of the circumference of the circle centered in $\vec{x}$ with radius $r = d_{\vec{x}\vec{y}}$ lying in C. An explicit expression is (see [32], p. 72)

$$w(\vec{x}, \vec{y}) = \begin{cases} 1 - \frac{1}{\pi} \sum_{k=1}^{2} \alpha(d_k) & \text{if } d_{\vec{x}\vec{y}}^2 \le \sum_{k=1}^{2} d_k^2 \text{ and} \\ \frac{3}{4} - \frac{1}{2\pi} \sum_{k=1}^{2} \beta(d_k) & \text{else,} \end{cases} \tag{1}$$

where

$$\alpha(t) = \cos^{-1}[\min(t, d_{\vec{x}\vec{y}})/d_{\vec{x}\vec{y}}],$$
$$\beta(t) = \cos^{-1}[t/d_{\vec{x}\vec{y}}],$$

and d_1 and d_2 are the distances of $\vec{x}$ to the nearest horizontal and vertical border, respectively, i.e., $d_1 = \min(x_1, 1 - x_1)$ and $d_2 = \min(x_2, 1 - x_2)$. Expression (1) is, however, only valid for $d_{\vec{x}\vec{y}} \le \frac{1}{2}$.

3.1.4. Inhomogeneity measure

We now propose an IM to assess the overall inhomogeneity of a point pattern based on Ripley's K-function that yields a value in the interval [0, 1]. The problem of applying $\widehat{K}$ directly is that it is not bounded because $w(\cdot, \cdot)$ can become very small and thus $1/w($

$\cdot, \cdot)$ very large. To attain a normalized measure of inhomogeneity we set

$$\widehat{K}^*(r, \mathcal{S}) = \min[1, \widehat{K}(r, \mathcal{S})],$$

integrate over the squared deviations of $\sqrt{\widehat{K}^*(r, \mathcal{S})/\pi}$ from the function $r \mapsto r$, and normalize it by

$$N_{\mathrm{K}} = \frac{\sqrt{18}\,(N-1) - N\left(6\sqrt{\frac{N-1}{N}\pi} - \sqrt{8\pi}\right)}{3N\pi},$$

resulting in Ripley's K-function IM

$$I_{\mathrm{K}}(\mathcal{S}) = \frac{1}{N_{\mathrm{K}}} \int_0^{\sqrt{2}} \left(\sqrt{\widehat{K}^*(r, \mathcal{S})/\pi} - r\right)^2 \mathrm{d}r. \tag{2}$$

The integration bounds are 0 and $\sqrt{2}$ since the maximum distance between any two points in the unit square C is $\sqrt{2}$.

Recall that (1) for evaluating $w(\cdot, \cdot)$ is only valid for $d_{\vec{x}\vec{y}} \leq \frac{1}{2}$, but we require an expression for $d_{\vec{x}\vec{y}} \leq \sqrt{2}$. Thus, we now present an expression valid for all such distances:

A weighting function valid for $d_{\vec{x}\vec{y}} > 0$ with $\vec{x}, \vec{y} \in C$ is

$$w(\vec{x}, \vec{y}) = \frac{\int_{\zeta_1}^{\zeta_2} \gamma(t)\,\mathrm{d}t + \int_{\zeta_3}^{\zeta_4} \gamma(t)\,\mathrm{d}t + \int_{\zeta_5}^{\zeta_6} \gamma(t)\,\mathrm{d}t + \int_{\zeta_7}^{\zeta_8} \gamma(t)\,\mathrm{d}t}{2\pi\, d_{\vec{x}\vec{y}}} \tag{3}$$

with

$$\gamma(t) = \sqrt{1 + \frac{(t - x_1)^2}{d_{\vec{x}\vec{y}}^2 - (t - x_1)^2}}$$

and the integration bounds

$$\zeta_1 = \zeta_5 = \max(0, x_1 - d_{\vec{x}\vec{y}}),$$

$$\zeta_2 = \max\left(0, x_1 - \mathrm{Re}\left(\sqrt{d_{\vec{x}\vec{y}}^2 - x_2^2}\right)\right),$$

$$\zeta_3 = \min\left(1, x_1 + \mathrm{Re}\left(\sqrt{d_{\vec{x}\vec{y}}^2 - x_2^2}\right)\right),$$

$$\zeta_4 = \zeta_8 = \min(1, x_1 + d_{\vec{x}\vec{y}}),$$

$$\zeta_6 = \max\left(0, x_1 - \mathrm{Re}\left(\sqrt{d_{\vec{x}\vec{y}}^2 - (1 - x_2)^2}\right)\right),$$

$$\zeta_7 = \min\left(1, x_1 + \mathrm{Re}\left(\sqrt{d_{\vec{x}\vec{y}}^2 - (1 - x_2)^2}\right)\right),$$

A proof of this result is given in Appendix A.

3.2. Discrepancy-based inhomogeneity measures

Discrepancy measures are used, for example, in statistical testing and numerical integration. In statistical testing, the aim is to place measurements uniformly (homogeneously) within the possible test space. In numerical integration, the discrepancies are applied to assess the differences between numerical and exact integrals. The following paragraphs describe five discrepancy measures from the literature and finally normalize them to fit into the range [0, 1].

The basic procedure of all of the following discrepancy measures is that the homogeneity of a point pattern is evaluated by integrating over local discrepancies D. Depending on the particular discrepancy measure, the measure is evaluated as either

$$\sqrt{\sum_{\mathcal{U} \neq \emptyset} \int_{C^{|\mathcal{U}|}} [D(\vec{x}^{\mathcal{U}})]^2\,\mathrm{d}\vec{x}^{\mathcal{U}}}, \tag{4}$$

or

$$\sqrt{\sum_{\mathcal{U} \neq \emptyset} \int_{C^{2|\mathcal{U}|}} [D(\vec{x}^{\mathcal{U}}, \vec{y}^{\mathcal{U}})]^2\,\mathrm{d}\vec{x}^{\mathcal{U}}\,\mathrm{d}\vec{y}^{\mathcal{U}}}, \tag{5}$$

where $\mathrm{d}\vec{x}^{\mathcal{U}} = \prod_{u \in \mathcal{U}} \mathrm{d}x_u$ and $\mathrm{d}\vec{y}^{\mathcal{U}} = \prod_{u \in \mathcal{U}} \mathrm{d}y_u$.

3.2.1. Star discrepancy

The key idea of the star discrepancy is as follows (see [36,37]): For a given point pattern, the local discrepancy is evaluated as the absolute difference between the area of a rectangle and the fraction of points contained in this rectangle.

Thus, the local discrepancy for given $\mathcal{U}$ and $\vec{x}^{\mathcal{U}}$ is

$$D_{\mathrm{S}}(\vec{x}^{\mathcal{U}}) = \left| \frac{|\mathcal{S}^{\mathcal{U}} \cap O(\vec{0}^{\mathcal{U}}, \vec{x}^{\mathcal{U}})|}{N} - \mathrm{Vol}(O(\vec{0}^{\mathcal{U}}, \vec{x}^{\mathcal{U}})) \right|.$$

The star discrepancy $\mathrm{S}(\mathcal{S})$ is then given according to (4) when replacing $D(\vec{x}^{\mathcal{U}})$ by $D_{\mathrm{S}}(\vec{x}^{\mathcal{U}})$. It is important to note that all regarded rectangles $O(\vec{0}^{\mathcal{U}}, \vec{x}^{\mathcal{U}})$ always originate from the point $\vec{0}^{\mathcal{U}}$. This explains also the name of the discrepancy measure. A closed-form expression for the star discrepancy is given as [38]

$$[\mathrm{S}(\mathcal{S})]^2 = \left(\frac{4}{3}\right)^2 - \frac{2}{N} \sum_{\vec{x} \in \mathcal{S}} \prod_{d=1}^{2} \left(\frac{3 - x_d^2}{2}\right) + \frac{1}{N^2} \sum_{\vec{x}, \vec{y} \in \mathcal{S}} \prod_{d=1}^{2} \left(2 - \max(x_d, y_d)\right).$$

3.2.2. Centered discrepancy

The centered discrepancy [39] is a modification of the star discrepancy such that it becomes invariant under reflections of $\mathcal{S}$ about any line $x_d = 0.5$, $d = 1, 2$. For each point $\vec{x} \in C$ it considers the rectangle defined by the point $\vec{x}$ and its closest corner (vertex) in C. Thus, formally, we have the following: Let $\mathcal{A} = \{(0, 0), (0, 1), (1, 0), (1, 1)\}$ be the set of all vertices of the observation area C. The local discrepancy is

$$D_{\mathrm{C}}(\vec{x}^{\mathcal{U}}) = \left| \frac{|\mathcal{S}^{\mathcal{U}} \cap O_{\vec{x}^{\mathcal{U}}}|}{N} - V(O_{\vec{x}^{\mathcal{U}}}) \right|.$$

The rectangle $O_{\vec{x}}$ is defined as

$$O_{\vec{x}} = O^*(\vec{a}^*, \vec{x}),$$

where $\vec{a}^* = \arg\min_{\vec{a} \in \mathcal{A}} d_{\vec{x}\vec{a}}$ and

$$O^*(\vec{a}, \vec{x}) = \begin{cases} O(\vec{a}, \vec{x}) & \text{if } \vec{a} \leq \vec{x}, \\ O(\vec{x}, \vec{a}) & \text{else.} \end{cases} \tag{6}$$

The centered discrepancy $\mathrm{C}(\mathcal{S})$ is then given by (4) replacing $D(\vec{x}^{\mathcal{U}})$ by $D_{\mathrm{C}}(\vec{x}^{\mathcal{U}})$. A closed-form expression for the centered discrepancy is [37]

$$[\mathrm{C}(\mathcal{S})]^2 = \left(\frac{13}{12}\right)^2 - \frac{2}{N} \sum_{\vec{x} \in \mathcal{S}} \prod_{d=1}^{2} \left(1 + \frac{1}{2}\left|x_d - \frac{1}{2}\right| - \frac{1}{2}\left|x_d - \frac{1}{2}\right|^2\right) + \frac{1}{N^2} \sum_{\vec{x} \in \mathcal{S}} \sum_{\vec{y} \in \mathcal{S}} \prod_{d=1}^{2} \left[1 + \frac{1}{2}\left|x_d - \frac{1}{2}\right| + \frac{1}{2}\left|y_d - \frac{1}{2}\right| - \frac{1}{2}\left|x_d - y_d\right|\right].$$

3.2.3. Symmetric discrepancy

The symmetric discrepancy [37] is, like the centered discrepancy, a reflection invariant discrepancy. Again, let $\mathcal{A}$ denote the set of all vertices of the observation area C. Then, any point $\vec{x} \in C$ divides the observation area into four rectangles, each defined by $\vec{x}$ and some $\vec{a} \in \mathcal{A}$. The discrepancy considers the so-called "even" rectangles, which are defined as the ones touching the vertex (0, 0) or (1, 1). The rectangle $O_{\vec{x}}$ is defined as the union of even rectangles, thus

$$O_{\vec{x}} = \bigcup_{a \in \{0,1\}} O^*((a, a), \vec{x}),$$

where $O^*(\vec{a}, \vec{x})$ is defined according to (6). The local discrepancy is given as

$$D_{\mathrm{Sym}}(\vec{x}^{\mathcal{U}}) = \left| \frac{|\mathcal{S}^{\mathcal{U}} \cap O_{\vec{x}^{\mathcal{U}}}|}{N} - V(O_{\vec{x}^{\mathcal{U}}}) \right|.$$

Table 1
Normalization factors .

X	S	C	Sym	U	W
N_X	$\frac{23}{18}$	$\frac{257}{288}$	$\frac{34}{9}$	$\frac{59}{288}$	$\frac{17}{36}$

The symmetric discrepancy $\mathrm{Sym}(\mathcal{S})$ is then given according to (4) when replacing $D(\vec{x}^{\mathcal{U}})$ by $D_{\mathrm{Sym}}(\vec{x}^{\mathcal{U}})$. A closed-form solution is given as [38]

$$[\mathrm{Sym}(\mathcal{S})]^2 = \left(\frac{4}{3}\right)^2 - \frac{2}{N}\sum_{\vec{x}\in\mathcal{S}}\prod_{d=1}^{2}\left(1+2x_d-2x_d^2\right) + \frac{1}{N^2}\sum_{\vec{x},\vec{y}\in\mathcal{S}}\prod_{d=1}^{2}(2-|x_d-y_d|). \tag{7}$$

3.2.4. Unanchored discrepancy

The unanchored discrepancy [38] does not require every rectangle to origin from $\vec{0}$ as it is the requirement of the star discrepancy. Instead, it considers the origin of rectangles by a parameter. Thus, the local discrepancy for $\mathcal{U}$ is

$$D_{\mathrm{U}}(\vec{x}^{\mathcal{U}},\vec{y}^{\mathcal{U}}) = \left|\frac{|\mathcal{S}^{\mathcal{U}}\cap O(\vec{x}^{\mathcal{U}},\vec{y}^{\mathcal{U}})|}{N} - V(O(\vec{x}^{\mathcal{U}},\vec{y}^{\mathcal{U}}))\right|$$

for given $\vec{x}^{\mathcal{U}},\ \vec{y}^{\mathcal{U}} \in C^{|\mathcal{U}|}$.

The unanchored discrepancy $\mathrm{U}(\mathcal{S})$ is then given according to (5) when replacing $D(\vec{x}^{\mathcal{U}},\vec{y}^{\mathcal{U}})$ by $D_{\mathrm{U}}(\vec{x}^{\mathcal{U}},\vec{y}^{\mathcal{U}})$. A closed-form expression for the unanchored discrepancy is [38]

$$[\mathrm{U}(\mathcal{S})]^2 = \left(\frac{13}{12}\right)^2 - \frac{2}{N}\sum_{\vec{x}\in\mathcal{S}}\prod_{d=1}^{2}\left(1+\frac{x_d(1-x_d)}{2}\right) + \frac{1}{N^2}\sum_{\vec{x},\vec{y}\in\mathcal{S}}\prod_{d=1}^{2}(1+\min(x_d,y_d)-x_dy_d). \tag{8}$$

3.2.5. Normalizing discrepancy-based measures

The mentioned discrepancy measures evaluate the homogeneousness of a point pattern by a non-normalized number; the smaller this number, the more homogeneous the point pattern is. We now normalize each of the discrepancies to obtain IM bounded in [0, 1].

For all discrepancies $X \in \{\mathrm{S}, \mathrm{C}, \mathrm{Sym}, \mathrm{U}, \mathrm{W}\}$, the corresponding IM is

$$I_X(\mathcal{S}) = \frac{X(\mathcal{S})}{\sqrt{N_X}},$$

where N_X denotes the normalization factor for discrepancy X. It is computed based on distributions yielding the maximum possible inhomogeneity for each measure. The normalization factors are shown in Table 1.

3.3. Grid-based inhomogeneity measure

The key idea of the grid-based IM [21] is to continuously partition the area C into subareas of ever-decreasing size. For each subarea, the *local deviation* is computed by comparing the number of points of $\mathcal{S}$ contained in this subarea to the expected number of points under a uniform distribution. The overall inhomogeneity measure of $\mathcal{S}$ is then a weighted sum over all local measures.

In the following we introduce the IM formally: Let the term *s-segmentation* denote a subdivision of the area C into s^2 subareas $C_i(s)$, $i = 1, 2, \ldots, s^2$, of equal size. Fig. 2(i) illustrates a 2-segmentation; Fig. 2(ii) shows a 4-segmentation.

For any given s-segmentation, the number of points contained in each subarea $C_i(s)$ is evaluated and compared to the expected number of points given a uniform distribution. The number of points contained in $C_i(s)$ is given as $|C_i(s)\cap\mathcal{S}|$, while the expected number of points under a uniform distribution is N/s^2. The deviation of $C_i(s)$ is defined as the absolute difference between these two numbers. Furthermore, we consider translations of $\mathcal{S}$ by defining the deviation of $C_i(s)$ as

$$\delta(C_i(s),\vec{x}) = \left||C_i(s)\cap\mathcal{S}_{\vec{x}}| - N/s^2\right|,$$

where $\mathcal{S}_{\vec{x}} = \{\vec{y}+\vec{x} \bmod 1 \mid \vec{y}\in\mathcal{S}\}$.

Then, the deviation of an entire s-segmentation is given as the maximum sum over the deviations $\delta(C_i(s),\vec{x})$, i.e.,

$$D_{\mathrm{G}}(s,\mathcal{S}) = \frac{1}{2N}\max_{\vec{x}\in C}\sum_{i=1}^{s^2}\delta(C_i(s),\vec{x}).$$

Property 1. *$D_{\mathrm{G}}(s,\mathcal{S})$ is bounded in [0, 1]. See Appendix B for the proof.*

Note that the area of $C_i(s)$ (see Fig. 2) is given as the set of points satisfying

$$\left\{(x_1,x_2)\in C \;\middle|\; \frac{\iota}{s}\le x_1 < \frac{\iota+1}{s},\quad \frac{\kappa}{s}\le x_2 < \frac{\kappa+1}{s}\right\},$$

where $\iota = (i-1) \bmod s$ and $\kappa = \lfloor (i-1)/s \rfloor$.

Finally, the overall grid-based IM of $\mathcal{S}$ is derived as the weighted sum of $D_{\mathrm{G}}(s,\mathcal{S})$, for $s = 2^1, 2^2, \ldots, 2^K$, i.e.,

$$I_{\mathrm{G}}(\mathcal{S}) = \sum_{k=1}^{K} w^{1-k} D_{\mathrm{G}}\left(2^k,\mathcal{S}\right). \tag{9}$$

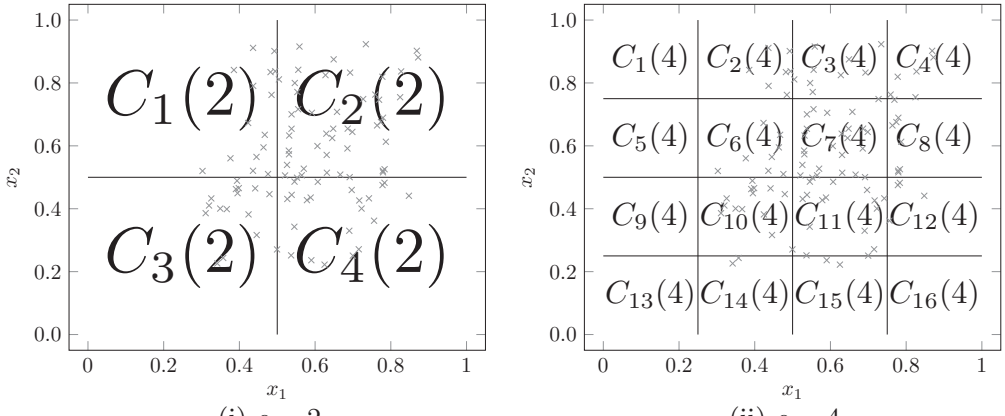

(i) $s = 2$ (ii) $s = 4$

Fig. 2. Examples of s-segmentations.

The value $K \in \mathbb{N} \cup \{\infty\}$ is the smallest positive number such that for all $\vec{x} \in C$ each subarea of the K-segmentation contains at most one point, i.e.,

$$\forall \vec{x} \in C: \ 1 \le i \ \le K^2 \Rightarrow |C_i(K) \cap \mathcal{S}_{\vec{x}}| \in \{0, 1\}. \tag{10}$$

If such a number does not exist, we have $K = \infty$. This situation occurs for point patterns $\mathcal{S}$ where at least two points are located at the same coordinate.

In both cases, however, (9) converges for appropriately chosen w. Moreover, we have the following property:

Property 2. *For* $w = \frac{5+\sqrt{21}}{2}$, *we have* $I_G(\mathcal{S}) \in [0, 1]$. *See Appendix B for the proof.*

In practical applications, large values of K increase the time required for the evaluation of (9) tremendously. Due to this, we replace K by

$$K^* = \min(K, 10),$$

such that only the first ten terms are considered. The contribution of higher terms to the outcome of the measure is negligible: In the worst case, where all the points of the point pattern are located at the same coordinate, the error is

$$\epsilon(N) = \sum_{k=11}^{\infty} w^{1-k} \frac{1}{2N} \left(N - \frac{N}{2^{2k}} + (2^{2k} - 1) \frac{N}{2^{2k}} \right).$$

It can be bounded by $\epsilon(N) < \sum_{k=11}^{\infty} w^{1-k} < 2 \cdot 10^{-7}$.

3.4. Extended wrap-around inhomogeneity measure

The extended wrap-around inhomogeneity measure, as suggested here, is based on the basic wrap-around discrepancy [38]. It allows, as the name implies, rectangles to wrap-around. The rectangles are defined as

$$O(\vec{x}^{\mathcal{U}}, \vec{y}^{\mathcal{U}}) = \bigtimes_{d \in \mathcal{U}}^{<} O_d(x_d, y_d),$$

where

$$O_d(x_d, y_d) = \begin{cases} [x_d, y_d] & \text{if } x_d \le y_d, \\ [0, y_d] \cup [x_d, 1] & \text{else.} \end{cases}$$

The local discrepancy is

$$D_W(\vec{x}^{\mathcal{U}}, \vec{y}^{\mathcal{U}}) = \left| \frac{|\mathcal{S}^{\mathcal{U}} \cap O(\vec{x}^{\mathcal{U}}, \vec{y}^{\mathcal{U}})|}{N} - V(O(\vec{x}^{\mathcal{U}}, \vec{y}^{\mathcal{U}})) \right|,$$

and the wrap-around discrepancy $W(\mathcal{S})$ is given according to (5) when replacing $D(\vec{x}^{\mathcal{U}}, \vec{y}^{\mathcal{U}})$ by $D_W(\vec{x}^{\mathcal{U}}, \vec{y}^{\mathcal{U}})$. A closed-form expression for the wrap-around discrepancy is [38]

$$[W(\mathcal{S})]^2 = -\left(\frac{4}{3}\right)^2 + \frac{1}{N^2} \sum_{\vec{x}, \vec{y} \in \mathcal{S}} \prod_{d=1}^{2} \left[\frac{3}{2} - |x_d - y_d| \cdot \left(1 - |x_d - y_d|\right) \right]. \tag{11}$$

The evaluation of the inhomogeneity measures (will be presented in Section 4) shows that the measures discussed so far exhibit either a very high computational effort (measure I_G) or have undesirable properties with respect to assessing inhomogeneity. For example, the wrap-around discrepancy I_W has a very low computational effort; it, however, fails for assessing the level of inhomogeneity (compare Fig. 3(c)). Thus, we propose a new IM combining the wrap-around IM I_W and Pearson's sample correlation coefficient ρ [40].

We define the extended wrap-around IM as

$$I_{EW}(\mathcal{S}) = \max\left[I_W(\mathcal{S}),\ I_W(\mathcal{S}_{\text{rot.}}),\ |\rho(\mathcal{S})|,\ |\rho(\mathcal{S}_{\text{rot.}})| \right], \tag{12}$$

where

$$\rho(\mathcal{S}) = \frac{\sum_{\vec{x} \in \mathcal{S}} (x_1 - \overline{\mathcal{S}^{\{1\}}}) \cdot (x_2 - \overline{\mathcal{S}^{\{2\}}})}{\sqrt{\sum_{\vec{x} \in \mathcal{S}} (x_1 - \overline{\mathcal{S}^{\{1\}}})} \sqrt{\sum_{\vec{x} \in \mathcal{S}} (x_2 - \overline{\mathcal{S}^{\{2\}}})}}$$

and $\mathcal{S}_{\text{rot.}}$ is the rotated point pattern emerging from $\mathcal{S}$ by applying algorithm A_R with angle $\phi = \pi/4$, i.e., $\mathcal{S}_{\text{rot.}} = A_R(\mathcal{S}, \pi/4)$. This algorithm is specified in Appendix C. Note that $\overline{\mathcal{S}^{\{\cdot\}}} = \frac{1}{|\mathcal{S}^{\{\cdot\}}|} \sum_{x \in \mathcal{S}^{\{\cdot\}}} x$.

4. Evaluation of inhomogeneity measures

This section evaluates the reviewed and presented IMs with respect to the following properties: (*A*) invariance against translation and rotation, (*B*) ability to assess inhomogeneity, (*C*) ability to assess homogeneity, and (*D*) computational complexity.

The following five algorithms are used for assessing the first two properties:

- *Translation* A_T. The points of the point pattern are moved by a given offset $\vec{o}$. Points exiting the observation area on one side reenter the area on the opposite side.
- *Rotation* A_R. The points are rotated by a specified angle ϕ. The axis of rotation is the center point of the observation area. Points exiting the observation area on one side reenter the area on the opposite side.
- *Move to center* A_C. The algorithm moves the points to the center point of the observation area. A parameter t ($0 \le t \le 1$) denotes the fraction of distance traveled from each point's initial position to the center point.
- *Move to horizontal line* A_H. The algorithm moves each point from its initial position to a randomly chosen point on the horizontal line crossing the center point of the observation area. A parameter t again denotes the fraction of distance travelled.
- *Move to diagonal line* A_D. The points of the point pattern move from their initial position to a randomly chosen point on the line connecting the points (0, 0) and (1, 1).

Further we assess property (*B*) by measuring the inhomogeneity of Matérn point processes (MPP) and determinantal point processes (DPP). A formal specification of these algorithms can be found in Appendix C.

4.1. Invariance against translation and rotation

In order to assess the invariance of the IMs with respect to translation and rotation, we proceed as follows:

1. We generate 100 point patterns $\mathcal{S}(i)$, $i = 1, \ldots, 100$, each having $N = 50$ points. Each point of the pattern is placed randomly and independently on C following a uniform distribution.
2. From each of these point patterns $\mathcal{S}(i)$ we generate two point patterns $\mathcal{S}(i, t)$ by moving the points according to Algorithm A_C with parameter $t = 0.5$ and $t = 1$.
3. For each of the point patterns generated in 2) we apply the translation algorithm A_T with uniformly chosen $\vec{o} \in [-\frac{1}{2}, \frac{1}{2}]^2$ and the rotation algorithm A_R with uniformly chosen angle $\phi \in [0, 2\pi]$, resulting in $\mathcal{S}_{\text{trans.}}(i, t)$ and $\mathcal{S}_{\text{rot.}}(i, t)$, respectively.
4. We quantify the impact of translation and rotation on the respective IM I_X by evaluating

   $$\varepsilon_{\text{trans.}}(I_X, i, t) = |I_X(\mathcal{S}(i, t)) - I_X(\mathcal{S}_{\text{trans.}}(i, t))|$$

   and

   $$\varepsilon_{\text{rot.}}(I_X, i, t) = |I_X(\mathcal{S}(i, t)) - I_X(\mathcal{S}_{\text{rot.}}(i, t))|.$$

   The smaller these ε-values are the more robust (invariant) the IM is.

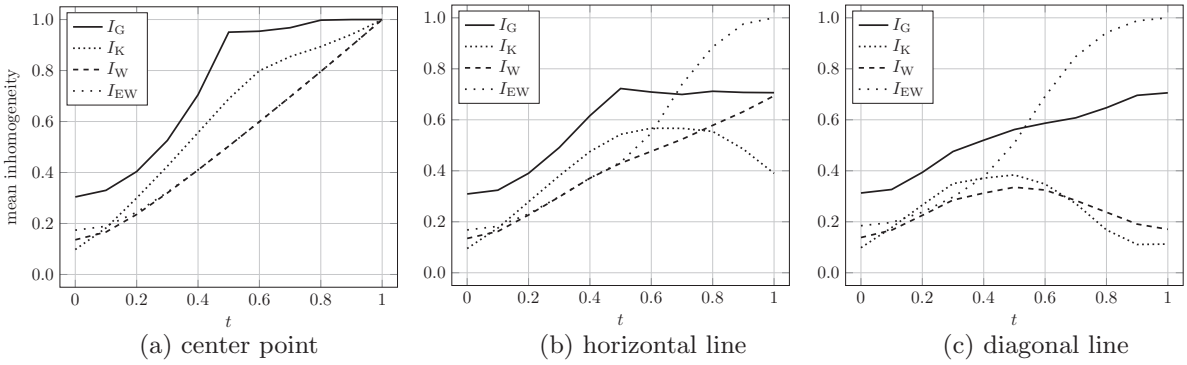

Fig. 3. Progression of inhomogeneity.

Table 2
Invariance with respect to translation and rotation.

Translation invariance $\varepsilon_{\text{trans.}}$											
	(i) $t = 0$				(ii) $t = 0.5$				(iii) $t = 1$		
	5% qu.	95% qu.	mean		5% qu.	95% qu.	mean		5% qu.	95% qu.	mean
I_K	0.000	0.069	0.016	I_K	0.021	0.590	0.375	I_K	0.000	0.000	0.000
I_W	0.000	0.000	0.000	I_W	0.000	0.000	0.000	I_W	0.000	0.000	0.000
I_U	0.000	0.005	0.002	I_U	0.003	0.033	0.023	I_U	0.004	0.077	0.043
I_G	0.000	0.000	0.000	I_G	0.000	0.000	0.000	I_G	0.000	0.000	0.000
I_C	0.001	0.050	0.019	I_C	0.006	0.180	0.091	I_C	0.021	0.425	0.204
I_S	0.001	0.047	0.018	I_S	0.003	0.163	0.075	I_S	0.012	0.346	0.158
I_{Sym}	0.001	0.025	0.010	I_{Sym}	0.021	0.150	0.098	I_{Sym}	0.019	0.332	0.177
I_{EW}	0.000	0.136	0.042	I_{EW}	0.000	0.200	0.030	I_{EW}	0.000	0.000	0.000
Rotation invariance $\varepsilon_{\text{trans.}}$											
	(i) $t = 0$				(ii) $t = 0.5$				(iii) $t = 1$		
	5% qu.	95% qu.	mean		5% qu.	95% qu.	mean		5% qu.	95% qu.	mean
I_K	0.000	0.111	0.043	I_K	0.000	0.012	0.005	I_K	0.000	0.106	0.045
I_W	0.001	0.078	0.024	I_W	0.000	0.015	0.005	I_W	0.001	0.074	0.025
I_U	0.001	0.071	0.023	I_U	0.000	0.013	0.004	I_U	0.001	0.067	0.023
I_G	0.001	0.133	0.047	I_G	0.000	0.187	0.087	I_G	0.001	0.135	0.049
I_C	0.000	0.049	0.017	I_C	0.000	0.009	0.003	I_C	0.001	0.052	0.018
I_S	0.001	0.045	0.017	I_S	0.000	0.010	0.004	I_S	0.001	0.049	0.018
I_{Sym}	0.000	0.013	0.004	I_{Sym}	0.000	0.003	0.001	I_{Sym}	0.000	0.014	0.005
I_{EW}	0.000	0.122	0.039	I_{EW}	0.000	0.015	0.005	I_{EW}	0.000	0.000	0.000

The results are given in Table 2. The measures I_W, I_{EW}, and I_G are highly invariant to translation. The measures I_U, I_C, I_S, and I_{Sym} are variant to translation, even if all points are located at the same location (case $t = 1$). The latter is an undesired property of an IM, since the level of inhomogeneity should be the same no matter where this location is. We thus exclude these four IMs from further analysis. All IMs are reasonably invariant against rotation. The measure I_{Sym} is the most invariant against rotation. For the measure I_{EW} all values are zero in the case $t = 1$.

4.2. Ability to assess inhomogeneity

An IM should yield values close to zero for homogeneous point patterns, and its value should increase the more inhomogeneous a point pattern is. In particular, the inhomogeneity of a point pattern should increase when all points move closer to some confined subspace of the overall area. To assess this progression of inhomogeneity, we use three examples of such subspaces: the center point of the area, a horizontal line crossing the center point, and a diagonal line between the points (0, 0) and (1, 1). Formally, we proceed in the following way:

1. We generate 100 point patterns $\mathcal{S}(i)$, $i = 1, \ldots, 100$, each having $N = 50$ points. Each point of the pattern is placed randomly and independently on C, following a uniform distribution.
2. From each of these point patterns $\mathcal{S}(i)$ we generate point patterns $\mathcal{S}_C(i, t) = A_C(\mathcal{S}(i), t)$ (center point), $\mathcal{S}_H(i, t) = A_H(\mathcal{S}(i), t)$ (horizontal line), and $\mathcal{S}_D(i, t) = A_D(\mathcal{S}(i), t)$ (diagonal line).
3. We evaluate the inhomogeneity values attributed to these point patterns by the measures. The mean inhomogeneities are shown in Fig. 3 for $0 \le t \le 1$.

Fig. 3(a) shows that if points move from their initial locations toward the center for a distance given by the fraction t, the mean inhomogeneity value of all measures increases with growing t. If points move toward a horizontal line (b) or a diagonal line, the mean inhomogeneity also first increases with growing t, but then again decreases for some IM with t growing further. The measures I_G and I_{EW} are the only IM whose inhomogeneity increases steadily, which is a desired property. The figure illustrates that now for all scenarios (center point, horizontal line and diagonal line) the value of the inhomogeneity measure I_{EW} increases. The increase of inhomogeneity value is furthermore much more linear with respect to t than for the other inhomogeneity measures. Further, as can be seen, at some ranges for t the measures I_{EW} and I_W are the same while for others they are different showing the regions in which the maximum in equation (12) is equal to $I_W(\mathcal{S})$.

4.3. Inhomogeneity of Matérn and determinantal point processes

Certain non-Poisson point processes play an important role for modeling wireless networks. Among these are the Matérn point processes (MPP) that are capable of capturing the properties of a network adopting carrier sensing for medium access [41].

MPP are hard-core processes that guarantee a minimum distance h between all pairs of points. There are different types of processes suggested by Matérn; we focus on type II, which yields the highest point density among all types of Matérn processes [34]. A realization of this process can be generated in the following way: First, a point pattern is generated from a PPP with intensity λ, and every point x is marked with a random number m_x of the interval (0, 1). Second, for every point x, it is checked whether or not there is a point y in the ball $B(x, h)$ for which $m_y < m_x$. If such point y exists, the point x is marked to be removed, otherwise it is retained. Third, all points that are marked to be removed are actually deleted. The set of retained points finally form the realization of the MPP. The intensity λ_M of the resulting MPP is given by [34]

$$\lambda_M = \frac{1 - \exp(-\lambda h^2 \pi)}{h^2 \pi} . \tag{13}$$

Fig. 4 shows the progression of inhomogeneity over different hard-core distances h averaged over 10 simulation runs for each point. It can be seen that the value of h has only little impact on inhomogeneity. In Fig. 4a the intensity of the Matérn process is fixed to $\lambda_M = 30$ by adjusting the intensity λ of the PPP for each value of h based on (13). Inhomogeneity values of all measures are slightly decreasing for increasing h, although for I_K this can hardly be seen from the plot. This effect can be explained by the dependent thinning applied for the MPP: For points of the PPP located in a dense region the survival probability is smaller than for points located in a sparse region. In the extreme case if a point has no nodes with a circle with radius h around it, it is retained with probability 1. Hence, random fluctuation of the density of points stemming from the PPP tend to be reduced by the thinning, leading to a more regular point pattern than that of the pristine PPP. This effect is stronger for higher values of h.

In Fig. 4b the intensity λ of the PPP is held constant leading to different intensities λ_M of the MPP. For $h = 0.05$ at the very left of the plot average intensity is $\lambda_M \approx 98$, i.e., almost all points of the PPP are retained and the curves show the inhomogeneity of the PPP itself. On the very right hand side the intensity is $\lambda_M \approx 34$ resembling the setup of Fig. 4a. Inhomogeneity values are slightly higher for higher values of h, which is only caused by the reduced number of points: When having fewer points, small random fluctuations of their locations show a stronger impact on the measured inhomogeneity leading to higher values.

Next, we measure the inhomogeneity of determinantal point processes (DPP). Fig. 5 shows the values of the inhomogeneity measures for different parameter values of DPPs. Fig. 5a and b show the inhomogeneity of the Whittle-Matérn determinantal point process; Fig. 5c and d show the inhomogeneity of the Bessel determinantal point process. What we can judge from these plots is that inhomogeneity does not depend on the parameters of these processes independent of the adopted measure.

4.4. Ability to assess homogeneity

To evaluate the impact of the number of points N on a given IM, we take the example of spatial point patterns sampled from a uniform distribution. We let the number of points range from $N = 10$ to 200. Fig. 6 shows the results. In particular, for I_G but also for I_W and I_{EW}, a small number of points increases the mean inhomogeneity significantly. The value of I_{EW} is always greater or equal to

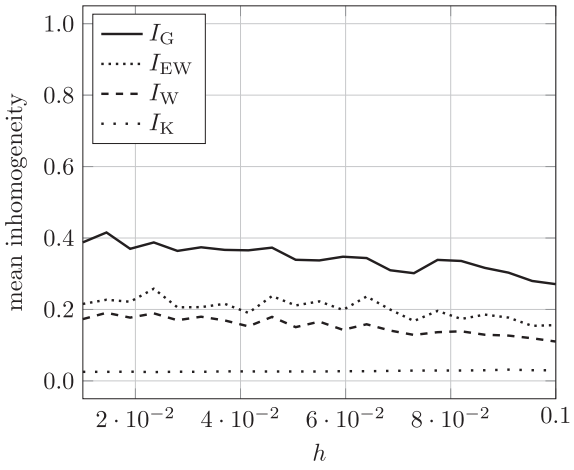

(a) Constant expected number of points intensity of the MPP is $\lambda_M = 30$.

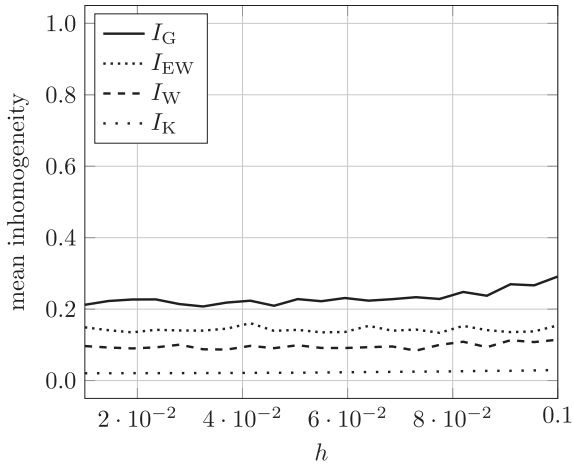

(b) Variable expected number of points. The PPP used for thinning has an intensity $\lambda = 100$.

Fig. 4. Inhomogeneity of Matérn point processes.

the value of I_W due to (12). For I_K this increase is also present but nowhere near as strong as for the other ones. The inhomogeneity values decrease for increasing N for all measures.

4.5. Computational complexity

The computational complexity classes of straightforward implementations of the algorithms with respect to the number of operations (addition, subtraction, multiplication etc.) are shown in Table 3.

A simple implementation of I_G requires $O(N^3)$ operations. For such an implementation the first and second coordinates of the points are first sorted separately, which can be done with $O(N \log(N))$ operations. These two sorted coordinate lists are the offsets that have to be considered. In particular, for each of these N^2 combinations of coordinates we translate the point pattern by the given offset, such that the coordinate lies in the upper left corner of the observation area C. Then for each of these translations, we determine for each point of the point pattern into which subinterval it falls. Thus, the overall computational effort is $O(N^3)$. The measure I_K requires the evaluation of a double sum requiring $O(N^2)$ operations. Furthermore, the edge correction factor $w(\cdot, \cdot)$ has to evaluated. Equation (3) requires the evaluation of four integrals. Numerical integration is independent of the number of

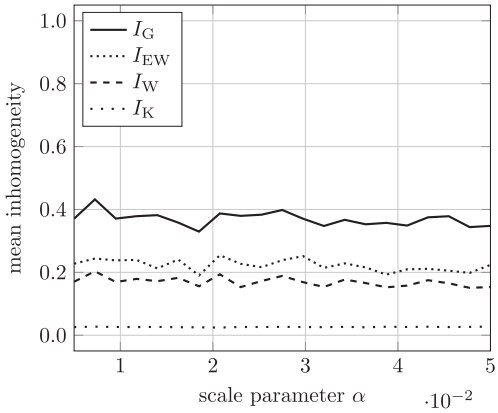

(a) Whittle-Matérn determinantal point process; intensity of the DPP is $\lambda_D = 30$ and the shape parameter $\nu = 1$.

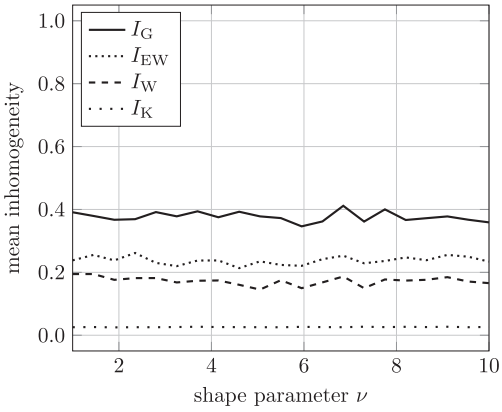

(b) Whittle-Matérn determinantal point process; intensity of the DPP is $\lambda_D = 30$ and the scale parameter $\alpha = 0.01$.

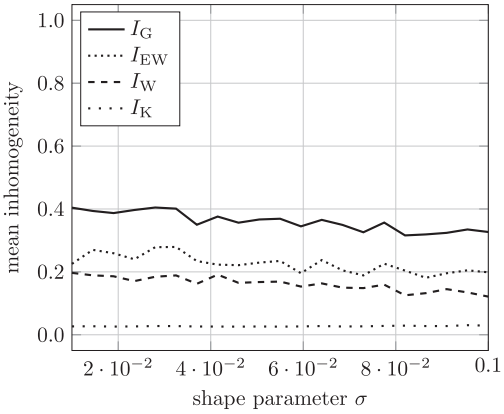

(c) Bessel determinantal point process; intensity of the DPP is $\lambda_D = 30$ and the scale parameter $\alpha = 1$.

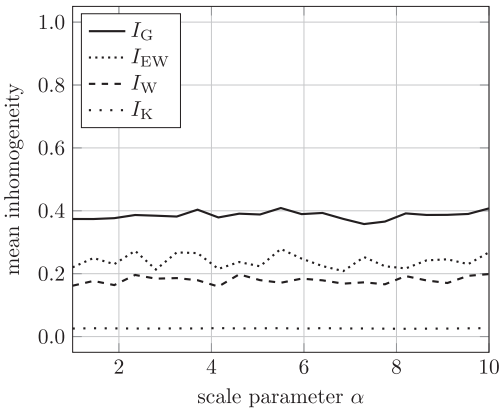

(d) Bessel determinantal point process; intensity of the DPP is $\lambda_D = 30$ and the shape parameter $\sigma = 0.01$.

Fig. 5. Inhomogeneity of determinantal point processes.

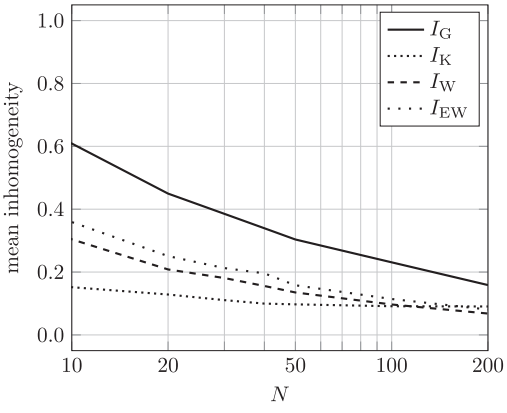

Fig. 6. Progression of homogeneity.

points N of the point pattern. Thus, the overall computational complexity is bounded by $O(N^2)$. Measure I_W requires the evaluation of equation (11), i.e., the evaluation of a double sum. Thus, the measure has a computational complexity of $O(N^2)$. We note that more sophisticated implementations can be applied reducing the computational effort to $O(N(\log(N))^2)$ [42]. The extended wrap-around measure I_{EW} requires the evaluation of two correlation coefficients and two double sums. Thus, the computational complexity is $O(N^2)$.

Table 4 shows execution times of the algorithms in practice. The measurements have been performed using a Intel Quad Core 2.4 GHz processor running Windows 7. The table shows the average execution durations in seconds, each based on 100 runs. Each run involves the calculation of the respective IM on a random spatial distribution. Note that the execution times are highly dependent on computer architecture and implementation. The values are shown as a qualitative comparison of execution times in practice. The table shows that for the measures I_W and I_{EW} the execution times are in the order of 10^{-4} s, depending on the number of points N. For the measures I_G and I_K the execution times are considerably higher reaching about 23 and 9 s for $N = 200$, respectively.

Table 3
Computational complexity.

I_G	I_K	I_W	I_{EW}
$O(N^3)$	$O(N^2)$	$O(N^2)$	$O(N^2)$

Table 4
Average execution times in seconds.

N	I_G	I_K	I_W	I_{EW}
50	0.30	0.55	$5.8 \cdot 10^{-6}$	$1 \cdot 10^{-5}$
100	2.59	2.19	$2.7 \cdot 10^{-5}$	$4 \cdot 10^{-5}$
200	23.03	8.78	$1.1 \cdot 10^{-4}$	$1.5 \cdot 10^{-4}$

Table 5
Summarizing the performance properties of the inhomogeneity measures.

Property	I_G	I_K	I_W	I_{EW}
Translation and rotation	Good	Good	Good	Good
Assess inhomogeneity	Good	Bad	Bad	Good
Inhomog. of MPP and DPP	Good	Bad	Good	Good
Assess homogeneity	Bad	Good	Medium	Medium
Computational complexity	$O(N^3)$	$O(N^2)$	$O(N^2)$	$O(N^2)$
Execution times	High	High	Low	Low

The results show that I_{EW} assesses the inhomogeneity of spatial points patterns very well, while at the same time exhibiting low computational effort in practice. Therefore, in the next section we apply I_{EW} as the inhomogeneity measure.

4.6. Summary

Table 5 summarizes the evaluation results of the inhomogeneity measures in a qualitative way.

5. Generation of inhomogeneous point patterns

In many applications we require spatial point patterns with a given inhomogeneity value. In this section we present and discuss a method to generate such point patterns. The presented approach is cluster-based and works in the following way:

1. We start with a point pattern where we randomly and uniformly place N points in the observation area C.
2. We choose $c \geq 1$ cluster points. The coordinates of these cluster points are again randomly and uniformly chosen from the observation area.
3. We randomly and uniformly assign to each of the N points of the point pattern one cluster point.
4. Each point moves from its initial position to its assigned cluster point, where a parameter $t \in [0, 1]$ determines the fraction of distance traveled.

Note that cluster points are not points of the point pattern. The parameters of the aforementioned procedure are c and t. The achievable inhomogeneity values depend on their values.

To analyze the achievable inhomogeneity values, we apply IM I_{EW} and plot the inhomogeneity values depending on c and t in Fig. 7.

The figure illustrates the mean inhomogeneity over 10 000 simulations for point patterns with $N = 50$ points. Furthermore, also the 5% and 95% quantiles are shown. The figure shows that the

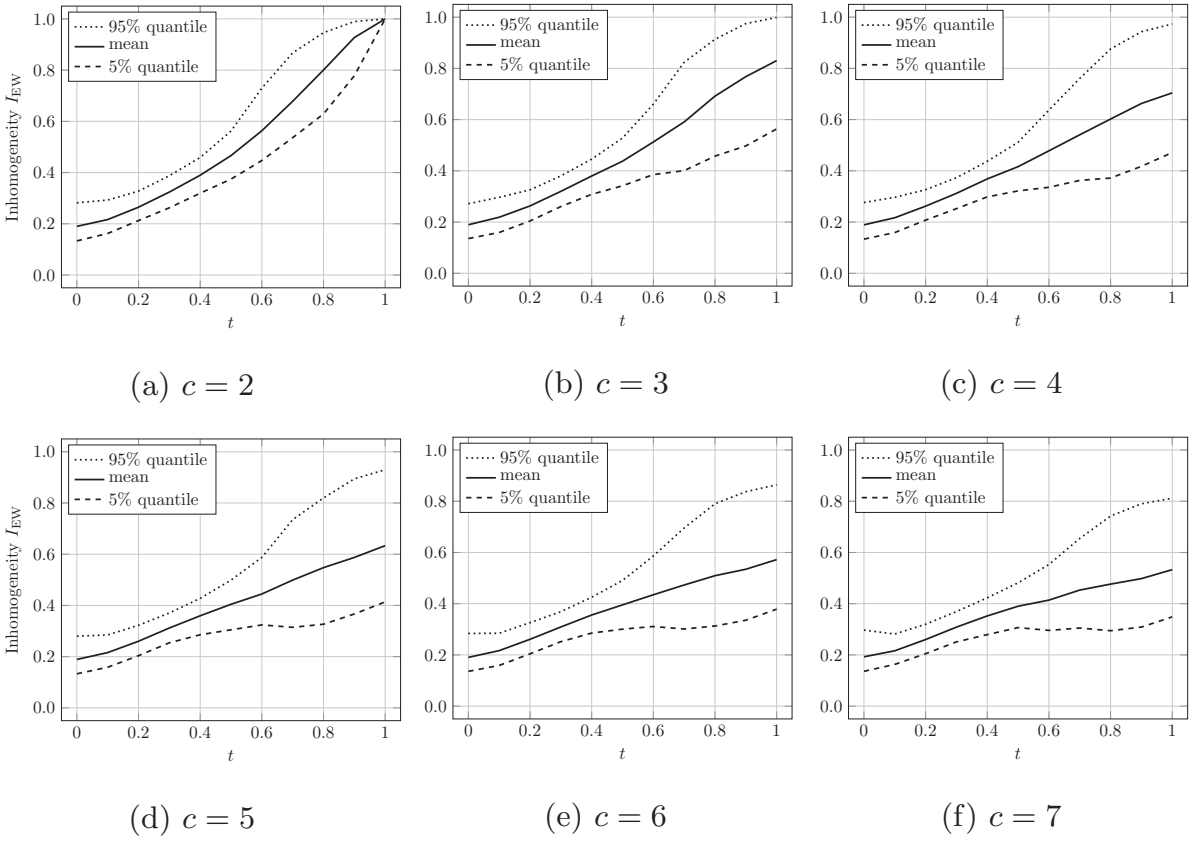

Fig. 7. Inhomogeneity values I_{EW} for cluster-based generation ($N = 50$).

Table 6
Cluster-based generation: independency of N .

t	$c=2$	3	4	5	6	7
0.0	0.06	0.05	0.05	0.05	0.05	0.05
0.1	0.04	0.04	0.04	0.04	0.05	0.04
0.2	0.03	0.03	0.03	0.03	0.03	0.04
0.3	0.02	0.03	0.03	0.03	0.02	0.02
0.4	0.02	0.02	0.02	0.02	0.02	0.02
0.5	0.01	0.02	0.02	0.02	0.03	0.02
0.6	0.01	0.01	0.02	0.02	0.03	0.03
0.7	0.01	0.03	0.03	0.02	0.04	0.04
0.8	0.02	0.04	0.02	0.03	0.03	0.05
0.9	0.01	0.04	0.04	0.02	0.03	0.03
1.0	0.00	0.03	0.04	0.03	0.02	0.02

Table 7
Average number of iterations $\overline{\eta}$ of Algorithm 2.

I^*	$c=2$	3	4	5	6	7
0.2 ($t=0.0$)	1.32	1.30	1.36	1.36	1.40	1.39
0.3 ($t=0.3$)	1.33	1.28	1.25	1.20	1.23	1.20
0.4 ($t=0.4$)	1.37	1.37	1.57	1.73	1.82	1.95
0.5 ($t=0.6$)	2.35	2.04	2.26	2.87	3.45	4.63
0.6 ($t=0.7$)	2.67	2.99	3.79	5.52	6.76	7.81
0.7 ($t=0.8$)	3.73	4.39	6.90	7.19	9.26	12.35
0.8 ($t=0.8$)	3.66	5.18	7.14	10.31	16.39	26.32
0.9 ($t=0.9$)	3.51	3.85	7.87	13.16	27.78	43.48

achievable inhomogeneity value decreases, with high probability, with increasing number of clusters points c: For $c=2$ cluster points we can achieve an inhomogeneity value of one, while for $c=7$ cluster points 95% of all inhomogeneity values are smaller than about 0.8. Note that the impact of the number of points N on the results is negligible: In Table 6 we show for each t and c the maximum deviations of the mean inhomogeneities for $\mathcal{N}=\{50, 60, 70, 80, 90, 100, 200, 1000\}$, formally given as

$$\max_{N_1,N_2\in\mathcal{N}} \frac{1}{1000}\left|\sum_{i=1}^{1000} I_{\mathrm{EW}}(\mathcal{S}(i,N_1,c,t)) - \sum_{j=1}^{1000} I_{\mathrm{EW}}(\mathcal{S}(j,N_2,c,t))\right|,$$

where $\mathcal{S}(i,N,c,t)$ denotes the ith point pattern with N points and parameters c and t, generated according to the procedure given above. Furthermore, also the deviations from the 5% and 95% quantiles are negligible (not shown in the table).

The algorithm to generate a spatial point pattern $\mathcal{S}$ with a given inhomogeneity value $I^*\in[0,1]$ such that

$$I_{\mathrm{EW}}(\mathcal{S})\in[I^*-\varepsilon, I^*+\varepsilon], \tag{14}$$

with $\varepsilon>0$, is given in Algorithm 2 (see Appendix D).

The parameters of the algorithm are the number of points N of the generated point pattern $\mathcal{S}$, the number of cluster points $c\geq 1$, the target inhomogeneity I^* and the deviation parameter $\varepsilon>0$. It is clear that the parameters c, I^* and ε have direct impact on the number of iterations η required to generate the point pattern satisfying constraint (14). In Table 7 we show for selected parameters the average number of iterations $\overline{\eta}$ taken by Algorithm 2 to generate a point pattern. The table illustrates that for, e.g., $I^*=0.9$ and $t=0.8$ the average number of iterations generally increases for increasing number of clusters. For $c=2$ it takes on average $\overline{\eta}=3.51$ iterations, while for $c=7$ this value increases to $\overline{\eta}=43.48$. In all cases we apply $\varepsilon=0.05$.

Finally, Fig. 8 illustrates samples of point patterns ($N=100$ points) generated with Algorithm 2.

6. Related work

6.1. Point processes and their statistical analysis

Many books are concerned with point processes [32,35,43,44]. A two volume edition covering many aspects of point processes, ranging from basic properties of Poisson processes to palm theory, is [45,46].

A comprehensive book about the statistical analysis of point patterns is [32]. The book covers, in depth, Ripley's K-function and its parameter estimation from given point patterns. Tests for complete spatial randomness are discussed and their applications illustrated on sample data.

Cressie [35] covers a wide range of methods for the statistical analysis of point patterns. The book addresses the analysis of geostatistical data and spatial point patterns in general. Tests for hypothesis testing with respect to, e.g., complete spatial randomness are discussed. Furthermore, the book also deals with Ripley's K-function.

6.2. Discrepancy measures in statistical testing and numerical integration

Two important application domains for discrepancy measures are the fields of statistical testing and numerical integration.

In the former application field it is the aim to find test plans where measurement samples are homogeneously distributed over the entire test space. The discrepancy measures are applied to assess the quality of test plans with respect to their homogeneousness. Manuscripts involving statistical testing and discrepancy measures are, e.g. [39,47,48].

In the latter application field, the field of numerical integration, discrepancy measures are applied to upper-bound the error of numerical integration. The Koksma-Hlawka inequality [36] is one of the most well-known multidimensional quadrature error bounds. It basically involves the star discrepancy as an integral component. Since then many other discrepancies have been proposed. Manuscripts about discrepancies and numerical integration include [37,49,50].

6.3. Assessing the (in-)homogeneity of spatial point patterns

A measure similar to the grid-based inhomogeneity measure is proposed by Zwicky in [51]. This measure, however, does not consider offsets and is therefore variant to linear operations.

Johansson et al. [52] applies kurtosis to measure the homogeneity of any property on a given area. The proposed approach requires some knowledge of the underlying distribution of the point pattern and is thus not applicable in our scenario.

Furthermore, many manuscripts are concerned with statistical hypothesis testing on whether or not a spatial distribution is homogeneous (see [53–55]). The output of such tests is, however, either the acceptance or the rejection of the hypothesis. These tests do not provide information on the level of inhomogeneity.

7. Conclusions

We have presented and extended methods for assessing the level of inhomogeneity of spatial point patterns and see this article as a service to researchers concerned with modeling and simulation of wireless networks and its associated requirement to adequately model real-life networks. Among these methods have been the discrepancy measures and Ripley's K-function, which are commonly applied in the fields of statistical testing and numerical integration. Evaluations of the measures have been performed to

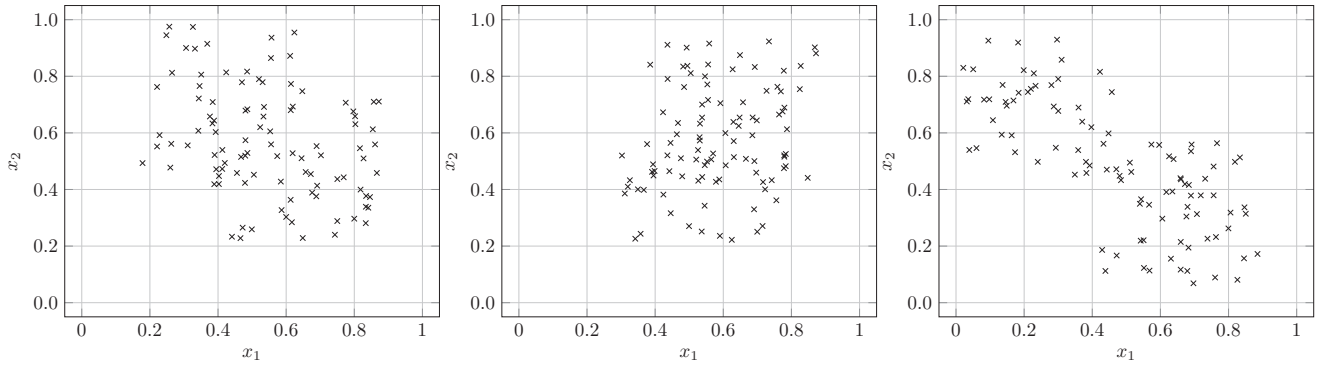

(i) $I_{\mathrm{EW}}(\mathcal{S}) = 0.36$ (ii) $I_{\mathrm{EW}}(\mathcal{S}) = 0.50$ (iii) $I_{\mathrm{EW}}(\mathcal{S}) = 0.72$

(a) $c = 2$, $t = 0.5$

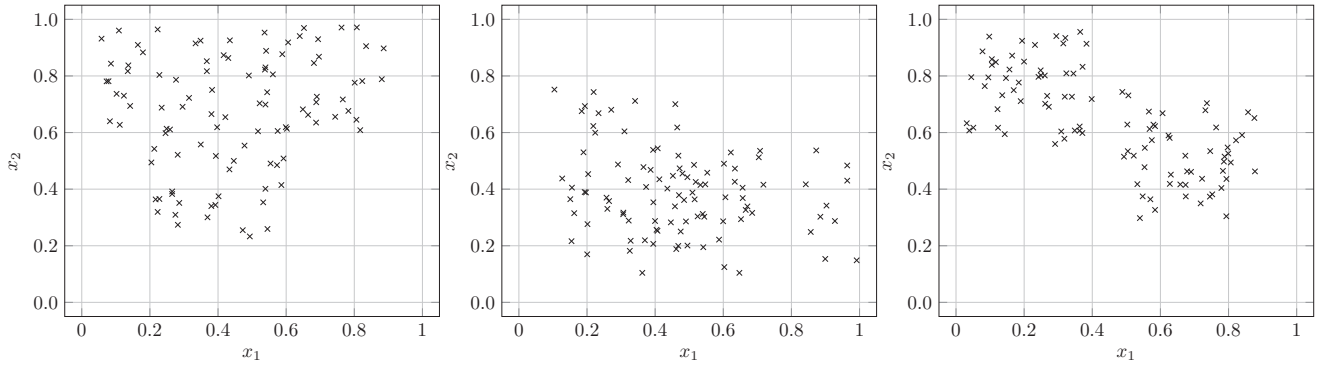

(i) $I_{\mathrm{EW}}(\mathcal{S}) = 0.33$ (ii) $I_{\mathrm{EW}}(\mathcal{S}) = 0.51$ (iii) $I_{\mathrm{EW}}(\mathcal{S}) = 0.68$

(b) $c = 4$, $t = 0.6$

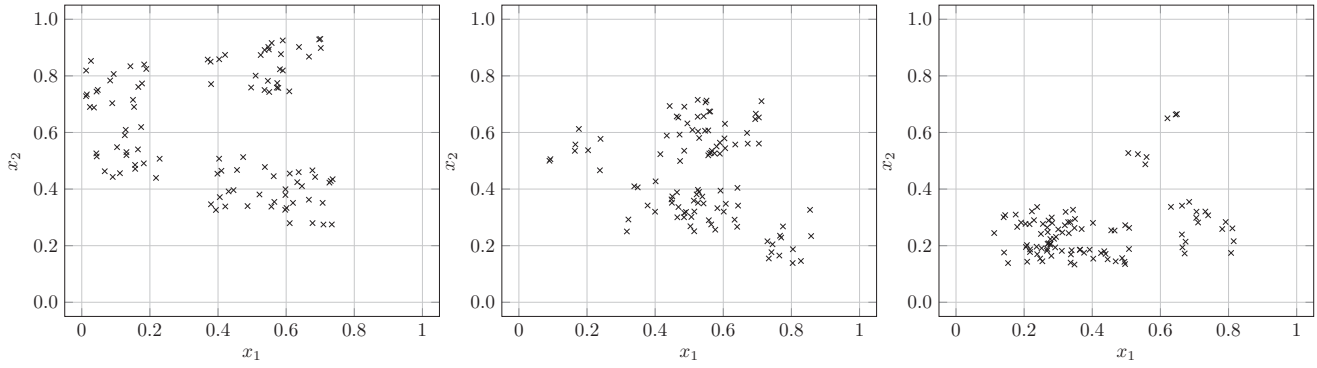

(i) $I_{\mathrm{EW}}(\mathcal{S}) = 0.32$ (ii) $I_{\mathrm{EW}}(\mathcal{S}) = 0.52$ (iii) $I_{\mathrm{EW}}(\mathcal{S}) = 0.72$

(c) $c = 7$, $t = 0.8$

Fig. 8. Samples of randomly generated inhomogeneous spatial point patterns ($N = 100$).

appraise their ability to assess the inhomogeneity of point patterns. Results have shown that these inhomogeneity measures are either incapable of assessing the inhomogeneity adequately, or exhibit an exceptionally high computational effort. Therefore, we proposed a novel inhomogeneity measure, the extended wrap-around discrepancy, which combines both low computational effort and proficiency in assessing a spatial point pattern's inhomogeneity. Finally, we have presented an algorithm to efficiently generate spatial point patterns exhibiting a specified level of inhomogeneity. This is an important contribution, as it is in general not easy to

synthesize point patters with certain inhomogeneity, in particular for higher inhomogeneity.

The result of our evaluation can be summarized as follows: As a general guideline, a researcher should choose the extended wrap-around measure for most applications, since it provides good ability to assess inhomogeneity at small computational cost. However, if elaborate theoretical investigations of the inhomogeneity of a point process are targeted, Ripley's K-function or the pair-correlation function would be a better choice. Finally, when computational cost is not important, the grid based approach is a good option since it very accurately assesses the inhomogeneity of a broad range of point patterns.

Acknowledgments

Work was supported by Lakeside Labs with funding from ERDF, KWF, BABEG under Grant 20214/23794/35530, and by FWF under grant P24480-N15.

Appendix A. Weighting function

Let w be the fraction of the circumference of the circle centered in $\vec{x} \in C$ with radius $d_{\vec{x}\vec{y}} = d(\vec{x}, \vec{y}) > 0$, which overlaps with the unit square C. We have

$$2\pi d_{\vec{x}\vec{y}} w = \int_{\zeta_1}^{\zeta_2} \gamma(t)\,\mathrm{d}t + \int_{\zeta_3}^{\zeta_4} \gamma(t)\,\mathrm{d}t + \int_{\zeta_5}^{\zeta_6} \gamma(t)\,\mathrm{d}t + \int_{\zeta_7}^{\zeta 8} \gamma(t)\,\mathrm{d}t,$$

where

$$\begin{aligned}
\zeta_1 &= \zeta_5 = \max(0, x_1 - d_{\vec{x}\vec{y}}),\\
\zeta_2 &= \max\left(0, x_1 - \mathrm{Re}\left(\sqrt{d_{\vec{x}\vec{y}}^2 - x_2^2}\right)\right),\\
\zeta_3 &= \min\left(1, x_1 + \mathrm{Re}\left(\sqrt{d_{\vec{x}\vec{y}}^2 - x_2^2}\right)\right),\\
\zeta_4 &= \zeta_8 = \min(1, x_1 + d_{\vec{x}\vec{y}}),\\
\zeta_6 &= \max\left(0, x_1 - \mathrm{Re}\left(\sqrt{d_{\vec{x}\vec{y}}^2 - (1-x_2)^2}\right)\right),\\
\zeta_7 &= \min\left(1, x_1 + \mathrm{Re}\left(\sqrt{d_{\vec{x}\vec{y}}^2 - (1-x_2)^2}\right)\right),\\
\gamma(t) &= \sqrt{1 + \frac{(t-x_1)^2}{d_{\vec{x}\vec{y}}^2 - (t-x_1)^2}}.
\end{aligned}$$

Proof. Let $r = d_{\vec{x}\vec{y}}$. Any circle can cross the boundaries of C at a maximum of eight points $\vec{v}_1$, $\vec{v}_2$, $\vec{v}_3$, $\vec{v}_4$, $\vec{v}_5$, $\vec{v}_6$, $\vec{v}_7$ and $\vec{v}_8$. Thus, we have to integrate over at most four arc segments of the circle. Consider the circle illustrated in Fig. A.9. For this circle, there are only five points on the circle that cross the boundaries of C. The points $\vec{v}_6$, $\vec{v}_7$ and $\vec{v}_4$, $\vec{v}_8$ each represent the same point.

The task is now to determine the projections of all $\vec{v}_i$ onto the first coordinate, i.e. $\zeta_i = \vec{v}_i^{\{1\}}$. We get:

(i) $\zeta_1 = \zeta_5 = \max(0, x_1 - r)$,

(ii) $\zeta_2 = \max\left(0, x_1 - \mathrm{Re}\left(\sqrt{r^2 - x_2^2}\right)\right)$,

(iii) $\zeta_3 = \min\left(1, x_1 + \mathrm{Re}\left(\sqrt{r^2 - x_2^2}\right)\right)$,

(iv) $\zeta_4 = \zeta_8 = \min(1, x_1 + r)$,

(v) $\zeta_6 = \max\left(0, x_1 - \mathrm{Re}\left(\sqrt{r^2 - (1-x_2)^2}\right)\right)$, and

(vi) $\zeta_7 = \min\left(1, x_1 + \mathrm{Re}\left(\sqrt{r^2 - (1-x_2)^2}\right)\right)$

Note that (i) and (iv) are derived in a straightforward manner (cf. Fig. A.9). For the derivation of (ii), (iii), (v) and (vi) we apply the Pythagorean theorem. In Fig. A.9 the derivation of (ii) is illustrated. The length s is given by $\sqrt{r^2 - x_2^2}$. In particular, the solution of this equation is imaginary if the circle does not intersect the boundaries of C; otherwise the solution is a real, possibly negative, number. Both cases are covered simultaneously by applying, in this case, $\max(0, \mathrm{Re}(\sqrt{r^2 - x_2^2}))$, where $\mathrm{Re}(x)$ denotes the real component of the complex number x.

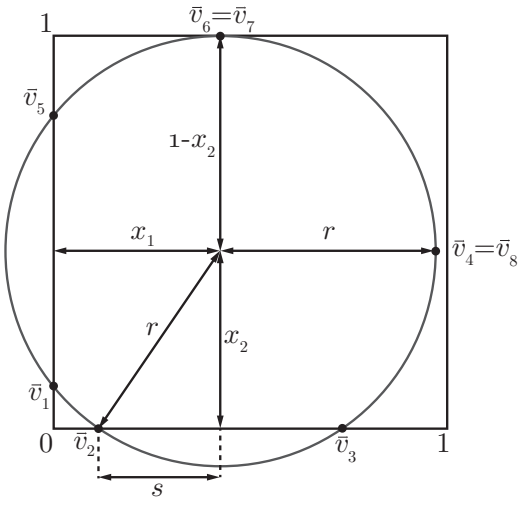

Fig. A.9. Example of a circle on the area C.

It remains to integrate over a maximum of four possible arc segments. Thus we have

$$\int_{\zeta_1}^{\zeta_2} \gamma(t)\,\mathrm{d}t + \int_{\zeta_3}^{\zeta_4} \gamma(t)\,\mathrm{d}t + \int_{\zeta_5}^{\zeta_6} \gamma(t)\,\mathrm{d}t + \int_{\zeta_7}^{\zeta 8} \gamma(t)\,\mathrm{d}t,$$

where

$$\gamma(t) = \sqrt{1 + \frac{(t-x_1)^2}{r^2 - (t-x_1)^2}}.$$

□

Appendix B. Grid-based inhomogeneity measure

Lemma 1. *$\sum_{i=1}^{s^2} \delta(C_i(s), \vec{x})$ is maximized for point patterns $\mathcal{S}$, where all N points are located at the same position.*

Proof. Assume that $N-1$ points of $\mathcal{S}$ are located at a given coordinate $\vec{y}$; the Nth point is located at another coordinate, however, sufficiently apart from $\vec{y}$, such that the $N-1$ points and the Nth point are contained in distinct subareas. Thus,

$$\begin{aligned}
\sum_{i=1}^{s^2} \delta(C_i(s), \vec{x}) &= \left|(N-1) - \frac{N}{s^2}\right| + \left|1 - \frac{N}{s^2}\right| + (s^2-2)\left|0 - \frac{N}{s^2}\right|\\
&< \left|N - \frac{N}{s^2}\right| + (s^2-1)\left|0 - \frac{N}{s^2}\right|.
\end{aligned}$$

The last line represents the value for a point pattern $\mathcal{S}$, where all nodes are located at the same coordinate. □

Property 1. *$D_{\mathrm{G}}(s, \mathcal{S})$ is bounded in* [0, 1].

Proof. The minimum of $D_{\mathrm{G}}(s, \mathcal{S})$ is reached, if all $\delta(C_i(s), \vec{x})$ are zero, i.e.,

$$\min_{\mathcal{S}} D_{\mathrm{G}}(s, \mathcal{S}) = \frac{1}{2N} \max_{\vec{x} \in C} \sum_{i=1}^{s^2} 0 = 0.$$

The maximum of $D_{\mathrm{G}}(s, \mathcal{S})$ is reached, if $\sum_{k=1}^{s^2} \delta(C_i(s), \vec{x})$ is maximized. This happens, as shown in Lemma 1, for point patterns $\mathcal{S}$, where all N points are located at the same position. Thus,

$$\begin{aligned}\max_{\mathcal{S}} D_{\mathrm{G}}(s,\mathcal{S}) &= \frac{1}{2N}\max_{\vec{x}\in C}\sum_{i=1}^{s^2}\delta(C_i(s),\vec{x})\\ &= \max_{\vec{x}\in C}\sum_{i=1}^{s^2}\frac{1}{2N}\delta(C_i(s),\vec{x})\\ &= \max_{\vec{x}\in C}\frac{1}{2N}\left[\left|N-\frac{N}{s^2}\right|+(s^2-1)\left|0-\frac{N}{s^2}\right|\right]\\ &= \max_{\vec{x}\in C}\frac{(s^2-1)}{s^2}\le 1.\end{aligned}$$

Furthermore, we have $\max_{\mathcal{S}}\lim_{s\to\infty} D_{\mathrm{G}}(s,\mathcal{S})=1$. □

Property 2. *For* $w=\frac{5+\sqrt{21}}{2}$, *we have* $I_{\mathrm{G}}(\mathcal{S})\in[0,1]$.

Proof. From Property 1 it follows that $\min_{\mathcal{S}} I_{\mathrm{G}}(\mathcal{S})=0$. For $\max_{\mathcal{S}} I_{\mathrm{G}}(\mathcal{S})$, we have

$$\begin{aligned}\max_{\mathcal{S}} I_{\mathrm{G}}(\mathcal{S}) &= \max_{\mathcal{S}}\sum_{k=1}^{K,} w^{1-k} D_{\mathrm{G}}(2^k,\mathcal{S})\\ &= \sum_{k=1}^{K} w^{1-k}\max_{\mathcal{S}} D_{\mathrm{G}}(2^k,\mathcal{S})\\ &= \sum_{k=1}^{\infty} w^{1-k}\frac{2^{2k}-1}{2^{2k}} = \sum_{k=1}^{\infty} w^{1-k}-\frac{w^{1-k}}{2^{2k}}\\ &= \frac{3w^2}{(w-1)(4w-1)}.\end{aligned}$$

For $w=\frac{5+\sqrt{21}}{2}$, we have $\frac{3w^2}{(w-1)(4w-1)}=1$. □

Data: $\mathcal{S}$, $\vec{o}$
Result: $\mathcal{S}'$
begin
  $\mathcal{S}' = \{\}$
  foreach $\vec{x}\in\mathcal{S}$ **do**
    $\vec{x}' = \vec{x} + \vec{o} \bmod 1$
    $\mathcal{S}' = \mathcal{S}' \cup \vec{x}'$
  end
end

(a) Translation A_T

Data: $\mathcal{S}$, ϕ
Result: $\mathcal{S}'$
begin
  $\mathcal{S}' = \{\}$
  foreach $\vec{x}\in\mathcal{S}$ **do**
    $\vec{x}' = \vec{x} - (1/2, 1/2)$
    $\vec{x}' = \vec{x}' \cdot \begin{matrix}\cos(\phi) & \sin(\phi)\\ -\sin(\phi) & \cos(\phi)\end{matrix}$
    $\vec{x}' = \vec{x}' + (1/2, 1/2) \bmod 1$
    $\mathcal{S}' = \mathcal{S}' \cup \vec{x}'$
  end
end

(b) Rotation A_R

Data: $\mathcal{S}$, t
Result: $\mathcal{S}'$
begin
  $\mathcal{S}' = \{\}$
  foreach $\vec{x}\in\mathcal{S}$ **do**
    $\vec{x}' = \vec{x} - [\vec{x} - (1/2, 1/2)]\cdot t$
    $\mathcal{S}' = \mathcal{S}' \cup \vec{x}'$
  end
end

(c) Move to center A_C

Data: $\mathcal{S}$, t
Result: $\mathcal{S}'$
begin
  $\mathcal{S}' = \{\}$
  foreach $\vec{x}\in\mathcal{S}$ **do**
    $x \sim \mathrm{U}(0,1)$
    $\vec{x}' = \vec{x} - [\vec{x} - (x, 1/2)]\cdot t$
    $\mathcal{S}' = \mathcal{S}' \cup \vec{x}'$
  end
end

(d) Move to horizontal line A_H

Data: $\mathcal{S}$, t
Result: $\mathcal{S}'$
begin
  $\mathcal{S}' = \{\}$
  foreach $\vec{x}\in\mathcal{S}$ **do**
    $x \sim \mathrm{U}(0,1)$
    $\vec{x}' = \vec{x} - [\vec{x} - (x, x)]\cdot t$
    $\mathcal{S}' = \mathcal{S}' \cup \vec{x}'$
  end
end

(e) Move to diagonal line A_D

Algorithm 1. Evaluation algorithms.

Data: N, c, t, I^*, ε
Result: $\mathcal{S}$ with $I_{\mathrm{EW}}(\mathcal{S}) \in [I^* - \varepsilon, I^* + \varepsilon]$
$\zeta = 0$
begin
  repeat
    randomly and uniformly generate a spatial distribution $\mathcal{S}$ with N points;
    randomly and uniformly place the c clusters in the observation area;
    assign each point $\vec{x} \in \mathcal{S}$ a cluster $\vec{c}_{\vec{x}} \in C$;
    for $\vec{x} \in \mathcal{S}$ **do**
      $\vec{x} = \vec{x} + (\vec{c}_{\vec{x}} - \vec{x}) \cdot t$
    end
    $\eta = \eta + 1$
  until $I_{EW}(\mathcal{S}) \in [I^* - \varepsilon, I^* + \varepsilon]$;
end

Algorithm 2. Cluster-based generation of inhomogeneous point patterns.

Appendix C. Algorithms to evaluate inhomogeneity measures

For the evaluation in Section 4 we apply five algorithms. They are formally specified in Algorithm 1 and discussed in the following.

- *Translation* A_T. The parameters of this algorithm are a point pattern $\mathcal{S}$ and an offset $\vec{o} \in \mathbb{R}^2$. The algorithm moves the points of the point pattern by the offset. The modulo operation ensures that points exiting the observation area C on one side reenter the area on the opposite side. The algorithm returns $\mathcal{S}'$ representing the translated point pattern.
- *Rotation* A_R. The parameters of this algorithm are the point pattern $\mathcal{S}$ and an angle $\phi \in [0, 2\pi)$. The algorithm rotates the points by the specified angle ϕ. The axis of rotation is the center point (0.5, 0.5) of the observation area C. This is done by first subtracting (0.5, 0.5) from all points in $\mathcal{S}$ and by multiplying each point with the rotation matrix. Finally, (0.5, 0.5) is again added to each point. The modulo operation ensures that points exiting the observation area on one side reenter it on the opposite side. The algorithm returns $\mathcal{S}'$ representing the rotated point pattern.
- *Move to center* A_C. The parameters of this algorithm are the point pattern $\mathcal{S}$ and a parameter $t \in [0, 1]$. The algorithm moves the points of the point pattern to the center point (0.5, 0.5) of the observation area C, where t denotes the fraction of distance travelled from each point's initial position to the center point. The algorithm returns $\mathcal{S}'$ representing the point pattern of moved points.
- *Move to horizontal line* A_H. The parameters of this algorithm are the point pattern $\mathcal{S}$ and a parameter $t \in [0, 1]$. The algorithm moves each point from its initial position to a point $(x, 0.5)$ lying on the horizontal line crossing the center point of the observation area. The value of x is randomly, uniformly and independently chosen for each point of the point pattern. The parameter t again denotes the fraction of distance travelled. The algorithm returns $\mathcal{S}'$ representing the point pattern of moved points.
- *Move to diagonal line* A_D. The parameters of this algorithm are the point pattern $\mathcal{S}$ and a parameter $t \in [0, 1]$. The points of the point pattern move from their initial position to a randomly, uniformly and for each point independently chosen point on the diagonal line connecting the points (0, 0) and (1, 1). The algorithm returns $\mathcal{S}'$ representing the point pattern of moved points.

Appendix D. Algorithm for cluster-based generation of inhomogeneous point patterns

A formal specification of the cluster[-]based generation of inhomogeneous point patterns is presented in Algorithm 2.

References

[1] A. Baier, K. Bandelow, Traffic Engineering and Realistic Network Capacity in Cellular Radio Networks with Inhomogeneous Traffic Distribution, in: Proc. IEEE Vehicular Technology Conference (VTC), 1997, pp. 780–784.
[2] C. Bettstetter, On the connectivity of ad hoc networks, Comput. J. 47 (4) (2004) 432–447. Oxford University Press
[3] S. Mukherjee, D. Avidor, Outage Probabilities in Poisson and Clumped Poisson-Distributed Hybrid Ad-hoc Networks, in: Proc. IEEE Conf. Sensor Ad Hoc Commun. Netw. (SECON), 2005, pp. 563–574.
[4] E. Perevalov, R. Blum, D. Safi, Capacity of clustered ad hoc networks: how large is "large"? IEEE Trans. Commun. 54 (9) (2006) 1672–1681.
[5] G. Alfano, M. Garetto, E. Leonardi, Capacity scaling of wireless networks with inhomogeneous node density: upper bounds, IEEE J. Select. Areas Commun. 27 (7) (2009) 1147–1157.
[6] G. Alfano, M. Garetto, E. Leonardi, V. Martina, Capacity scaling of wireless networks with inhomogeneous node density: lower bounds, IEEE/ACM Trans. Netw. 18 (5) (2010) 1624–1636.
[7] B. Ghosh, Random distances within a rectangle and between two rectangles, Bull. Calcutta Math. Soc. 43 (17–24).
[8] S. Srinivasa, M. Haenggi, Distance distributions in finite uniformly random networks: theory and applications, IEEE Trans. Veh. Technol. 59 (2) (2010) 940–949.
[9] D. Avidor, S. Mukherjee, Hidden issues in the simulation of fixed wireless systems, Wirel. Netw. 7 (2) (2001) 187–200.
[10] R. Vilzmann, J. Widmer, I. Aad, C. Hartmann, Low-Complexity Beamforming Techniques for Wireless Multihop Networks, in: Proc. IEEE Conf. Sensor Ad Hoc Commun. Netw. (SECON), volume 2, 2006, pp. 489–497.
[11] C. Bettstetter, M. Gyarmati, U. Schilcher, An Inhomogeneous Node Distribution and Its Stochastic Properties, in: Proc. ACM/IEEE Intern. Symp. on Modeling, Analysis, and Simulation of Wireless and Mobile Systems (MSWiM), Chania, Greece, 2007, pp. 400–404.
[12] D.B. Johnson, D.A. Maltz, Dynamic Source Routing in Ad Hoc Wireless Networks, in: T. Imielinski, H. Korth (Eds.), Mobile Computing, 1996, pp. 153–181. Springer US
[13] C. Bettstetter, G. Resta, P. Santi, The node distribution of the random waypoint mobility model for wireless ad hoc networks, IEEE Trans. Mobile Comput. 2 (3) (2003) 257–269.
[14] J. Yoon, M. Liu, B. Noble, Random Waypoint Considered Harmful, in: Proc. IEEE Conf. on Computer Communications (INFOCOM), 2003, pp. 1312–1321.
[15] W. Navidi, T. Camp, Stationary distributions for the random waypoint mobility model, IEEE Trans. Mobile Comput. 3 (1) (2004) 99–108.
[16] C. Bettstetter, H. Hartenstein, X. Pérez-Costa, Stochastic properties of the random waypoint mobility model, ACM Wireless Netw. 10 (5) (2004) 555–567.

[17] J.-Y.L. Boudec, On the stationary distribution of speed and location of random waypoint, IEEE Trans. Mobile Comput. 4 (4) (2005) 404–405.
[18] E. Hyytia, P. Lassila, J. Virtamo, Spatial node distribution of the random waypoint mobility model with applications, IEEE Trans. Mobile Comput. 5 (6) (2006) 680–694.
[19] B.-J. Kwak, N.-O. Song, M. Miller, A mobility measure for mobile ad hoc networks, IEEE Commun. Lett. 7 (8) (2003) 379–381.
[20] X. Peréz-Costa, C. Bettstetter, H. Hartenstein, Toward a mobility metric for comparable and reproducible results in ad hoc networks research, ACM Mobile Comput. Commun. Rev. 7 (4) (2003) 58–60.
[21] U. Schilcher, M. Gyarmati, C. Bettstetter, Y.W. Chung, Y.H. Kim, Measuring Inhomogeneity in Spatial Distributions, in: Proc. IEEE Vehicular Technology Conf. (VTC), 2008, pp. 2690–2694. Marina Bay, Singapore
[22] B.D. Ripley, The second-order analysis of stationary points processes, J. Appl. Probab. 13 (1976) 255–266.
[23] B.D. Ripley, Modelling spatial point patterns, Journal of the Royal Statistical Society, Series B 39 (1977) 172–192.
[24] M. Haenggi, R. Smarandache, Diversity polynomials for the analysis of temporal correlations in wireless networks, IEEE Trans. Wireless Commun. 12 (11) (2013) 5940–5951. Available at http://www.nd.edu/~mhaenggi/pubs/twc13d.pdf.
[25] U. Schilcher, G. Brandner, C. Bettstetter, Diversity Schemes in Interference-Limited Wireless Networks with Low-cost Radios, in: Proc. Wireless Commun. Networking Conf. (WCNC), 2011, pp. 707–712. Cancun, Mexico.
[26] U. Schilcher, S. Toumpis, A. Crismani, G. Brandner, C. Bettstetter, How Does Interference Dynamics Influence Packet Delivery in Cooperative Relaying? in: Proc. ACM/IEEE Intern. Conf. on Modeling, Analysis and Simulation of Wireless and Mobile Systems (MSWiM), 2013, pp. 347–354. Barcelona, Spain
[27] N. Deng, W. Zhou, M. Haenggi, The ginibre point process as a model for wireless networks with repulsion, IEEE Trans. Wireless Commun. 14 (2015) 107–121.
[28] M. Haenggi, Mean interference in hard-core wireless networks, IEEE Commun. Lett. 15 (8) (2011) 792–794. Available at http://www.nd.edu/~mhaenggi/pubs/cl11.pdf.
[29] S.S. Szyszkowicz, H. Yanikomeroglu, A simple approximation of the aggregate interference from a cluster of many interferers with correlated shadowing, IEEE Trans. Wireless Commun. 13 (8) (2014) 4415–4423.
[30] A. Guo, M. Haenggi, R.K. Ganti, SIR Asymptotics in General Network Models, CoRR abs/1611.04704 (2016) arXiv:1611.04704.
[31] M.M. Deza, E. Deza, Encyclopedia of distances, Springer, 2009.
[32] P.J. Diggle, Statistical analysis of spatial point patterns, Academic Press, 1983.
[33] K.T. Fang, X. Lu, P. Winker, Lower bounds for centered and wrap-around L2-discrepancies and construction of uniform designs by threshold accepting, J. Complex. 19 (5) (2003) 692–711.
[34] D. Stoyan, W.S. Kendall, J. Mecke, Stochastic geometry and its applications, 2nd edition, Wiley, 1995.
[35] N.A.C. Cressie, Statistics for spatial data, John Wiley & Sons, Inc., 1993.
[36] E. Hlawka, Funktionen von beschränkter variation in der theorie der gleichverteilung, Ann. Mat. Pura Appl. 54 (1961) 325–333.
[37] F.J. Hickernell, A generalized discrepancy and quadrature error bound, Mathematical Computing 67 (1998) 299–322.
[38] F.J. Hickernell, Random and Quasi-random Point Sets, in: Ch. Lattice rules: How well do they measure up?, volume 138, 1998, pp. 109–166. Springer-Verlag
[39] K.-T. Fang, C.-X. Ma, P. Winker, Centered L2-discrepancy of random sampling and latin hypercube design, and construction of uniform designs, Math. Comput. 71 (2000) 275–296.
[40] K. Pearson, Notes on Regression and Inheritance in the Case of Two Parents, in: Proc. Royal Society of London, volume 58, 1895, pp. 240–242.
[41] F. Baccelli, B. Błaszczyszyn, Stochastic Geometry and Wireless Networks, volume II: Applications, now publishing, 2009.
[42] S. Heinrich, Efficient algorithms for computing the L_2-discrepancy, Math. Comput. 65 (1996) 1621–1633.
[43] D.R. Cox, Point processes, monographs on statistics & applied probability (book 12), Chapman & Hall / CRC, 1980.
[44] D.L. Snyder, Random point processes in time and space, 2nd edition, Springer, 1991.
[45] D.J. Daley, D. Vere-Jones, An introduction to the theory of point processes, volume I, 2nd edition, Springer, 2003.
[46] D.J. Daley, D. Vere-Jones, An introduction to the theory of point processes, volume II, 2nd edition, Springer, 2007.
[47] K.-T. Fang, The uniform design: application of number-theoretic methods in experimental design, Acta Math. Appl. Sinica 3 (1980) 363–372.
[48] K.-T. Fang, C.-X. Ma, Wrap-around L2-discrepancy of random sampling, latin hypercubes and uniform designs, J. Complex. 17 (2001) 608–624.
[49] I.H. Sloan, Lattice methods for multiple integration, J. Comput. Appl. Math. 12–13 (1985) 131–143.
[50] F.J. Hickernell, Quadrature error bounds with applications to lattice rules, SIAM J. Numer. Anal. 33 (1997) 1995–2016.
[51] F. Zwicky, Morphological astronomy, Springer, 1957.
[52] J.-O. Johansson, Measuring homogeneity of planar point-patterns by using kurtosis, Pattern Recognit. Lett. 21 (2000) 1149–1156.
[53] J. Antoch, D. Jarušková, Testing a homogeneity of stochastic processes, Kybernetika 43 (4) (2007) 415–430.
[54] L.B. Collins, A. Pluzhnikov, M.L. Stein, Improvement of inter-event distance tests of randomness in spatial point processes, The University of Chicago, Department of Statistics, 1994 Technical report. http://www.dtic.mil/docs/citations/ADA291151, accessed May 26, 2015.
[55] R. Fierro, A. Tapia, Testing homogeneity for poisson processes, Revista Colombiana de Estadística 34 (3) (2011) 421–432.

Udo Schilcher studied applied computing and mathematics at the University of Klagenfurt, where he received two Dipl.-Ing. Degrees with distinction (2005, 2006). Since 2005, he has been research staff member at the Networked and Embedded Systems institute at the University of Klagenfurt. His main interests are interference and node distributions in wireless networks. His doctoral thesis on inhomogeneous node distributions and interference correlation in wireless networks and has been awarded with a Dr. techn. degree with distinction in 2011. He received a best paper award from the IEEE Vehicular Technology Society.

Günther Brandner received the Dipl.-Ing. degree (with distinction) in applied computing and mathematics from the University of Klagenfurt, Klagenfurt, Austria, in 2007 and 2008. Since 2007, he has been a research and teaching staff member and doctoral student with the Networked and Embedded Systems Institute, University of Klagenfurt. His main interests are relay selection methods for cooperative relaying and the implementation and evaluation of protocols on hardware platforms.

Christian Bettstetter received the Dipl.-Ing. degree in electrical engineering and information technology and the Dr.-Ing. degree (summa cum laude) in electrical engineering and information technology from the Technische Universität München (TUM), Munich, Germany, in 1998 and 2004, respectively. He was a Staff Member with the Communications Networks Institute, TUM, until 2003. From 2003 to 2005, he was a Senior Researcher with the DOCOMO Euro-Labs. Since 2005, he has been a Professor and the Head of the Institute of Networked and Embedded Systems, University of Klagenfurt, Klagenfurt, Austria. He is also the Scientific Director and Founder of Lakeside Labs, Klagenfurt: a research cluster on self-organizing networked systems. He coauthored the textbook GSM-Architecture, Protocols and Services (Wiley). Dr. Bettstetter received Best Paper Awards from the IEEE Vehicular Technology Society and the German Information Technology Society (ITG).